

ENVIRONMENTAL FACTORS AFFECTING THE HAZEL LANDSLIDE

LEVEL 2 WATERSHED ANALYSIS
HAZEL, WASHINGTON

Dan Miller and Joan Sias



M2 Environmental Services

Summary

This study uses physically based models of evapotranspiration, groundwater flow, and slope stability to evaluate the relative importance of different environmental factors affecting activity of the Hazel landslide. We find:

Clearcut logging increases recharge of groundwater flowing to the landslide. The time-averaged increase in recharge lies somewhere between 17% to 51% of the mean annual precipitation, and is most likely near the upper end of this range. This increase results primarily from a reduction in winter interception and the loss of winter transpiration.

Increased groundwater flow to the landslide reduces stability over some areas of the landslide. Rising watertables affect the landslide in a spatially variable fashion: some areas are not affected at all, others experience a large reduction in stability. The rise of the mean annual watertable caused by clearcut logging of the groundwater recharge area of the landslide results in reductions of the calculated mean annual factor of safety from zero to over 30%, depending on where one looks. Larger increases in recharge affect larger proportions of the landslide.

Clearcut logging in the groundwater recharge area of the landslide increases the proportion of time the landslide spends in a potentially unstable state. Stability of the landslide varies over time in response to changing groundwater levels. A persistent increase in recharge leads to a persistent reduction in stability. Over the 60-year climate record, a simulation for forested conditions results in a condition of failure 3% of the time (for the slope transect examined, failure involves slow movement of a flow-like slump). An increase in time-averaged recharge of 17% (the smallest estimated change between forested and clearcut conditions) resulted in a condition of failure 26% of the time.

Groundwater levels respond to annual levels of precipitation. A series of dry years may draw aquifer storage down to an extent that several years of average to above average precipitation are required to bring the watertable back up to average levels. Likewise, groundwater levels may remain elevated for a year or more following a series of wet years.

Incision of channels draining the landslide can also reduce stability. The reduction in the calculated factor of safety varies in value over the landslide from zero to a maximum of about 15%. Increased groundwater flow to the landslide will increase base flow through these channels, potentially increasing the mean annual flux of sediment carried by these channels to the Stillaguamish.

Bank erosion of the landslide toe reduces landslide stability. The reduction in the calculated factor of safety varies in value over the landslide from zero to a maximum of near 75% at points near the toe. *Bank erosion at the toe can destabilize the landslide over its entire length.*

Each of these processes affects different parts of the landslide, with some overlap. Historic landslide activity correlates well with areas predicted to be sensitive to one or more of these processes. Slumps at the toe are predicted to occur primarily in response to bank erosion; movement over the body of the landslide is predicted to occur in response to all three processes. Headward expansion of the landslide towards Headache Creek occurs in response to both bank erosion of the toe and incision of channels draining the landslide.

Clearcut logging outside of the groundwater recharge area can affect landslide stability, but the effect is minor. The shape and extent of the groundwater recharge area is influenced by spatial variations in recharge, but a worse-case scenario indicates low potential for destabilization of the landslide.

The results of this study indicate that movement of the Hazel landslide occurs in response to natural processes: landsliding will continue even in the absence of landuse. The results also indicate that clearcut logging in the groundwater recharge area of the landslide will accelerate landslide activity and increase the flux of sediment into the Stillaguamish River. As with any scientific inquiry, we cannot unambiguously prove these conclusions; we can only disprove them. Empirical correlations between the location and timing of clearcut harvests and landslide activity support (in that they do not disprove) these results. In this study we do not examine harvest techniques other than clearcutting.



Contents

Section 1. Introduction	1.1
The Hazel Landslide: Site Characterization	1.2
Historic Landslide Activity	1.6
References	1.9
Section 2. Simulation of Groundwater Recharge at Hazel in Relation to Vegetation Cover	2.1
Overview of Approach and Major Results	2.2
Model Description	2.3
Meteorological Data	2.4
Results	2.5
A. Average annual water balance	2.5
B. Time series of soil moisture	2.8
C Sensitivity analysis	2.8
Discussion	2.10
Conclusions	2.13
Impacts of Harvest on Steep Slopes with Thin Soils versus Low-gradient Slopes with Thick Soils	2.14
Thinning	2.14
Recommendations	2.15
Appendix I. Model description, parameter estimation	2.16
Interception loss	2.16
Aerodynamic resistance	2.16
Soil moisture accounting	2.17
Leaf area index (LAI)	2.17
Stomatal resistance	2.17
Winter application	2.18
Parameter values - clearcut	2.18
Appendix II. Estimation of meteorological forcing data at Hazel	2.19
Bibliography	2.20
Section 3. Stability Assessment of the Hazel Landslide	3.1
The Groundwater Model	3.1
Data requirements: Site Characterization	3.1
Simulated recharge	3.3
Calculated quantities	3.3
The Groundwater Recharge Area	3.4
The Stability Model	3.6
Spatial Patterns of Slope Stability	3.7
Sensitivity to Changes in Recharge	3.7
Sensitivity to Cutting of the Slope Toe	3.9
Sensitivity to Channels Incised over the Body of the Landslide	3.11
Discussion	3.12

Contents (continued)

Temporal Patterns of Slope Stability	3.12
Empirical Comparison	3.17
Effects of Toe Cutting	3.15
Effects of Harvest	3.15
Recharge on Steep, Bedrock Slopes with Thin Soils verses Low-gradient Slopes with Thick Soils	3.16
Summary	3.16
Resources and Tasks Required for Similar Analyses	3.17
References	3.18
Addendum: Effects of Clearcutting Outside of the Groundwater Recharge Area...	3.20

Environmental Factors Affecting the Hazel Landslide Level 2 Watershed Analysis, Hazel WAU

Dan Miller and Joan Sias

Introduction

This study seeks to identify and quantify the relative importance of environmental factors affecting a large landslide near Steelhead Haven along the North Fork of the Stillaguamish River (near river-mile 20), commonly known as the Hazel landslide. These results augment those of the Level 1 watershed analysis for the Hazel WAU (DNR, in prep). This work was funded by a contract from the Department of Ecology (contract # C9600040), administered by the Tulalip Tribes of Washington State, with information provided by Jeff Grizzel at the Northwest Regional office of the Department of Natural Resources (DNR) and digital topographic data provided by the DNR office in Olympia. Paul Kennard and Lee Benda provided pre-1991 aerial photographs.

The Hazel landslide is classified as a “large, persistent, deep-seated” landslide for purposes of watershed analysis (Washington Forest Practices Board, 1995) and has a documented history of movement extending from at least the early 1950s (Shannon and Associates, 1952; Benda et al., 1988). Material mobilized by deep-seated landslides can compose a significant portion of the sediment flux into a channel system (e.g., Collins et al., 1994), yet the environmental factors controlling such landslides are not well characterized. Several studies have cited apparent correlations between the timing of nearby timber harvest and landslide activity for this (Benda et al., 1988) and nearby (Benda and Collins, 1992; Kennard and Pess, 1994) sites with time lags of 5 to 20 years between timber removal and landslide movement, suggesting that increases in groundwater recharge following timber harvest (e.g., Wolff et al., 1989) can, at least in some cases, increase landslide activity. Such observations, although implicating timber removal, are not easily rendered into prescriptions for management at these or other sites. Likewise, other factors affecting landslide activity may also be involved, confounding any conclusions relating timber harvest and landsliding. For example, Benda et al. (1988) and DNR (in prep) note bank erosion at the toe of this and other landslides as a factor contributing to landslide initiation and continuing instability.

This study applies newly developed computational tools to assess environmental controls on deep-seated landsliding within the context of Washington State watershed analysis. It differs from previous studies in that, in addition to empirical observations, we characterize landslide behavior using physically based numerical models of evapotranspiration, groundwater flow, and landslide movement. These models utilize regional weather data, topography of the site, and subsurface stratigraphy estimated from field mapping of surface contacts to calculate estimates of the following quantities:

- a time series of groundwater recharge based on the given climate and site vegetation;
- the associated groundwater flow field; and
- slope stability, determined as a factor of safety, for all points over the area of interest (at the resolution of the topographic data).

With these calculated quantities we estimate spatial and temporal variations of landslide stability and the relative role of different controlling factors. Specifically, we estimate the potential impact of timber harvesting within the groundwater recharge area and examine the relative importance of pore-pressure changes associated with changes in recharge, incision of channels draining the body of the landslide, and erosion of the landslide toe by the Stillaguamish River. This allows us to address three questions posed by the Level 1 analysis team:

- 1) What is the relative importance of bank erosion into the toe of the slope versus increases in groundwater flux to the slope for initiating and or accelerating movement of the landslide?
- 2) What is the groundwater recharge area of the landslide?
- 3) How does evapotranspiration vary spatially? That is, will timber harvest from thin soils mantling steep bedrock slopes within the groundwater recharge area of a landslide have a different effect than harvest from deep soils on low-gradient slopes?

The first two questions are addressed directly; the third is examined in light of model results. In seeking answers to such questions, the methods described here allow us to use available information to a much greater extent than do empirical observations alone.

This report is divided into three sections. The Hazel site is described in this introduction. The second section, written by Joan Sias, describes the method she has developed to calculate a time series of at-a-point groundwater recharge using regional climatic data and site-specific vegetation. The third section, written by Dan Miller, describes the groundwater and slope stability models used for landslide assessment.

The Hazel Landslide

The Hazel landslide sits at the southeast end of the Whitman Bench (Figure 1.1), a large terrace remnant of the glacially-associated valley-filling deposits (lacustrine clays underlying glacial-fluvial outwash) typical of river valleys draining west from the Cascade crest to Puget Sound (Booth, 1989; Tabor et al., 1988). Post-glacial fluvial incision into these deposits has created conditions conducive to mass wasting. Morphology indicative of large, deep-seated landsliding is common throughout this region and, although most landslide deposits appear to be currently stable, several recently and currently active deep-seated landslides indicate the continuing potential for reactivation of old and initiation of new landslides in this material (e.g., Thorsen, 1989). Several large, post-glacial slump blocks scallop the margins of the Whitman Bench. As shown in Figure 1.2, the Hazel landslide is itself contained within one of these blocks and topography indicative of adjacent slumps occurs to the west and to the north. Indeed, Headache Creek basin appears to have been created by movement of a large slump east towards Rollins Creek.

These slumps probably occurred as the Stillaguamish and its tributaries incised the glacial deposits. The topographic relief created by incision provided the gravitational potential to drive large slumps downslope. That potential still exists. When and where landslides occur is thus controlled by continuing alterations to slope geometry, as when bank erosion cuts into a slope toe, and by variations in pore pressures. Pore pressures vary with changes in groundwater. An increase in groundwater flow to a slope is generally associated with decreased slope stability and increased potential for landsliding (see e.g., Freeze and Cherry, 1979). Landslide occurrence may be closely associated with regional and local patterns of groundwater flow and with changes in those patterns over time.

Groundwater flow to the Hazel landslide is controlled by local topography and stratigraphy. The source of groundwater is infiltration of rainfall and snowmelt from the surface. The movement of groundwater is driven by variations in head, i.e., by spatial variation of the watertable (in unconfined aquifers) or the potentiometric surface (in confined aquifers). In essence, groundwater flows “downhill” from areas of high head to areas of low head. The rate of flow is controlled by the hydraulic conductivity of the subsurface material. In general, recharge increases head (raises the watertable in an unconfined aquifer) so that groundwater flows from areas of recharge towards areas of discharge, which are typically seeps on slopes where an aquifer intersects the ground surface. (It is flow of groundwater, and its seepage to the surface into channels, that maintains summer baseflow in streams. In unconfined (watertable) aquifers, streams and ponds are points where the watertable intersects the ground surface.)

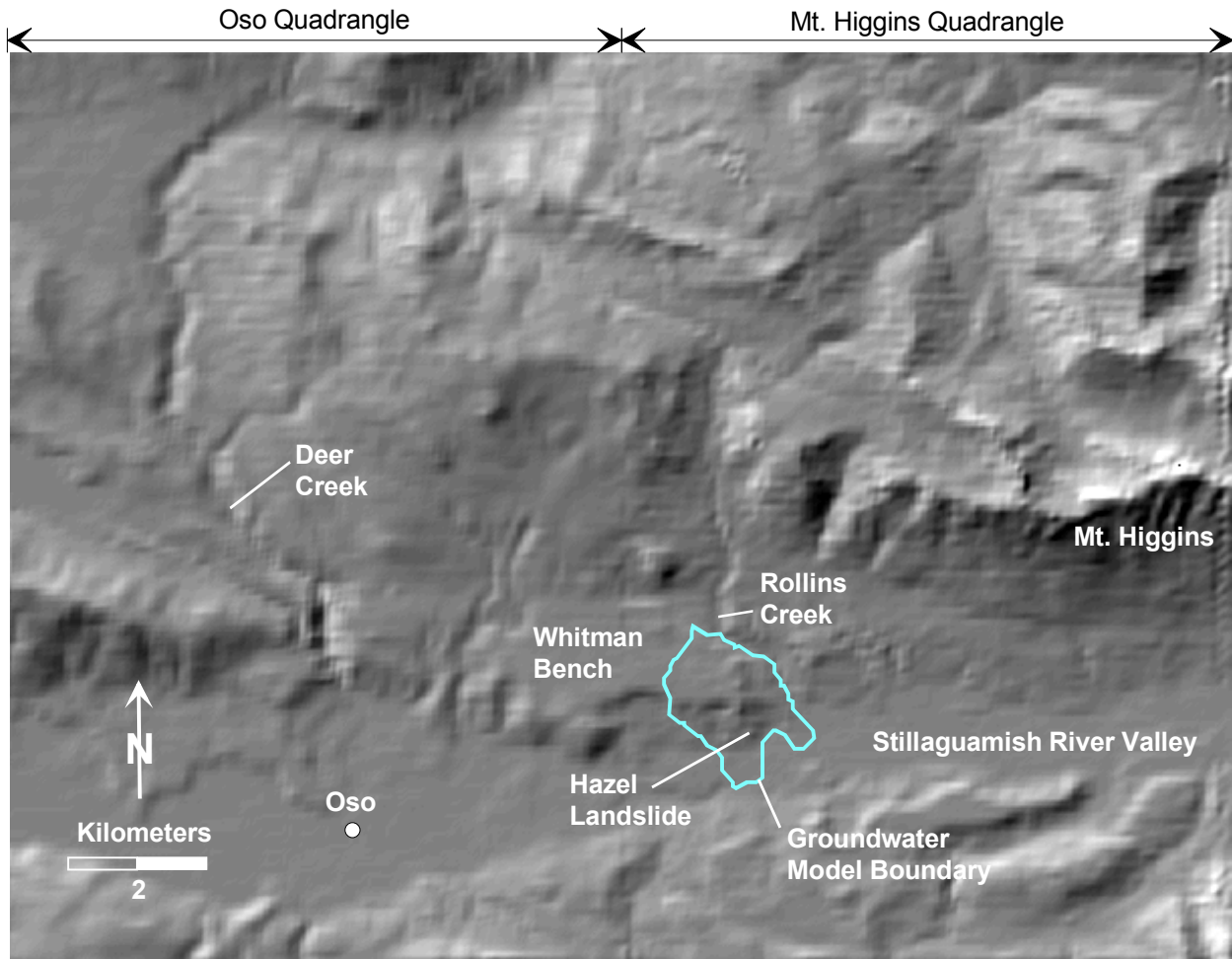


Figure 1.1. Shaded relief image of U.S.G.S. Oso and Mt. Higgins 7½-minute topographic quadrangles illustrating regional topography for the Hazel landslide. The groundwater model boundary is shown for reference in Section 2 of this report.

As seen in Figure 1.1, there is a large upslope area potentially contributing groundwater recharge to the Whitman Bench, extending all the way up the side of Mt. Higgins and into the headwaters of Deer Creek. The Hazel landslide may, however, be isolated from this pattern of regional groundwater flow by Rollins Creek (see also Figure 1.2), which defines the eastern edge of the Whitman Bench and veers slightly westward north of the landslide, so that the southeastern edge of the Whitman Bench forms a roughly triangular promontory at the margin of the Stillaguamish floodplain, with the Hazel landslide at its tip. Seepage observed along this length of Rollins Creek, even at the end of the summer dry season, indicates it is an effluent channel with groundwater flowing towards it from both the Mt. Higgins and Whitman Bench sides. Thus we infer that groundwater flowing towards the Hazel landslide comes entirely from recharge on the Whitman Bench. (We have no rigorous test of this inference; any well water levels from the Whitman Bench would prove very useful in this regard.)

The locations of surface seeps along the margins of the Whitman Bench allow us thus to infer a relatively simple groundwater flow system for the Hazel landslide, as illustrated in 1.3. The outwash sands create a

Hazel

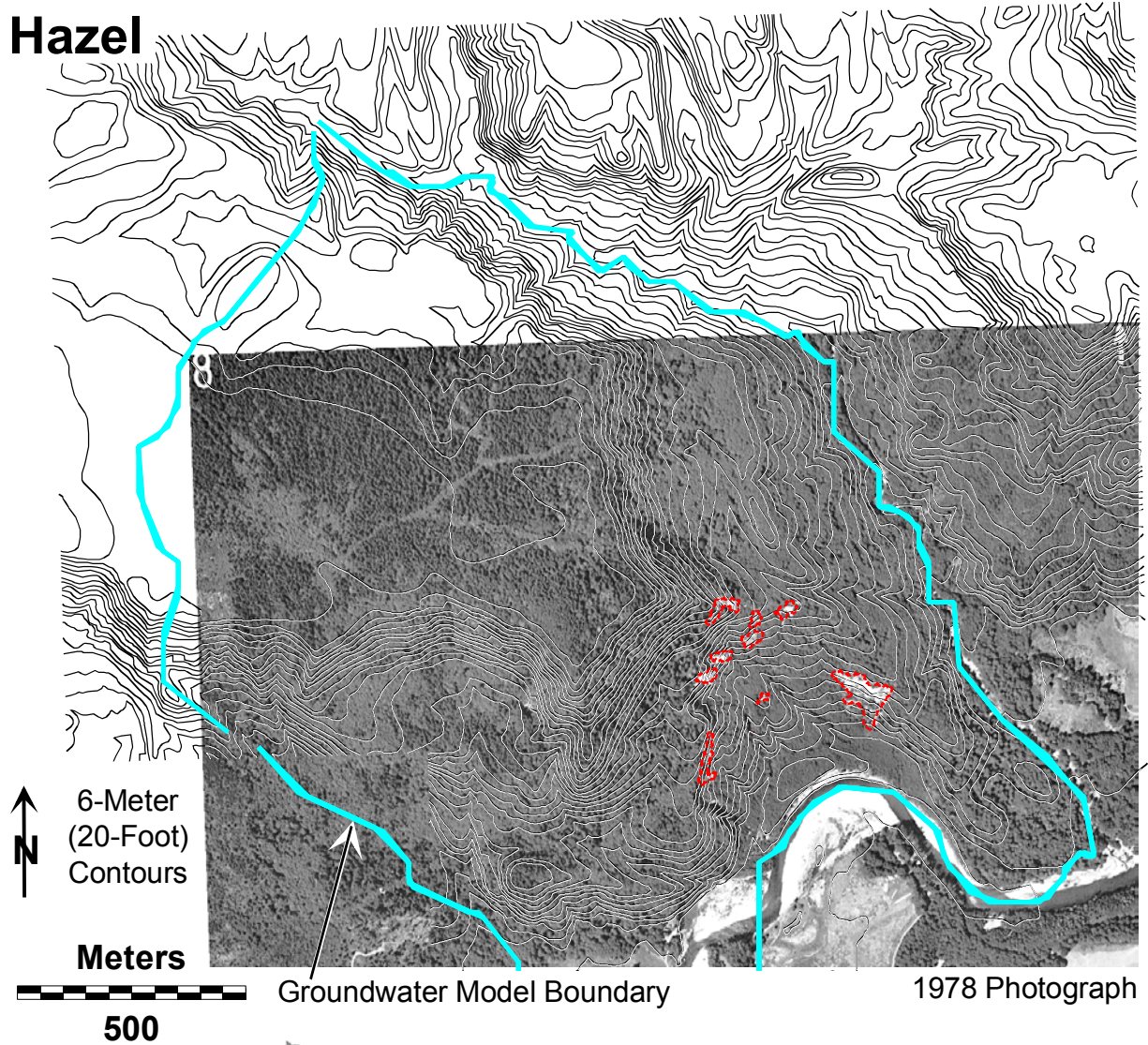
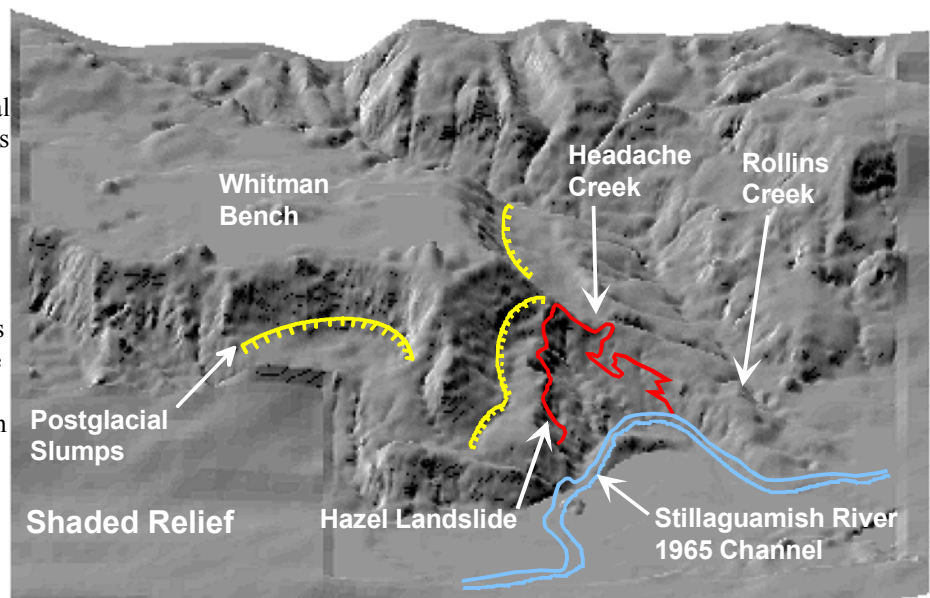


Figure 1.2. Site topography. Contour lines are based on 1978 aerial photography. Heavy red lines indicate zones of landslide activity visible in the 1978 photograph. The heavy blue line delineates the boundary of the groundwater model described in Section 3 of this report. Right is a perspective view of a portion of the shaded relief image shown in Figure 1.1, looking due north. The Hazel landslide and adjacent slump blocks are delineated.



permeable unconfined aquifer overlying the lacustrine clays, which because of their much lower permeability relative to the sands serve as an underlying aquiclude. Groundwater flows through the sands above the clay contact towards surface seeps along slopes draining to the Stillaguamish. Groundwater levels are determined by the permeability of the sand and the rate of recharge. Increasing recharge causes groundwater levels to rise, thus increasing the head gradient (watertable slope) towards the surface seeps, which causes the rate of groundwater flow to increase. Groundwater levels respond directly to variations in recharge. This response, however, is modulated by the rate at which groundwater flows to and through the aquifer (i.e., by the permeability of the sands). A transient increase in recharge may cause watertable levels to rise fairly quickly, over the course of several weeks to months. It may then take some time, several months to years, for this additional water to flow through the system to the areas of discharge – the surface seeps.

Variations in recharge correspond to variations in precipitation and evapotranspiration. Averaged over several years, recharge is equal to precipitation minus evapotranspiration. Over shorter terms, pore spaces in the soil serve as temporary stores of moisture. A well-drained soil (soil above the watertable) will hold a certain volume of the water draining through it because of surface tension of the water coating soil grains. This water is available to plant roots. Thus soil water is replenished during periods of rainfall and depleted by plant transpiration between rainstorms. As rains resume in the fall, the soil moisture must be replenished before recharge to groundwater occurs. The volume of water to be replenished is a function of soil characteristics and the rooting depth of plants.

The volume of water evaporated and transpired is a function of local climate and of vegetation characteristics. Evapotranspiration is found to be greater over forests than over clearcuts (see e.g., Wolff et al., 1989). Thus, vegetation in the recharge area of this aquifer will influence watertable levels and, to the extent that groundwater controls slope stability, will influence landslide activity. We examine these effects in sections two and three of this report, but first we examine the history of activity and harvest for the Hazel landslide.

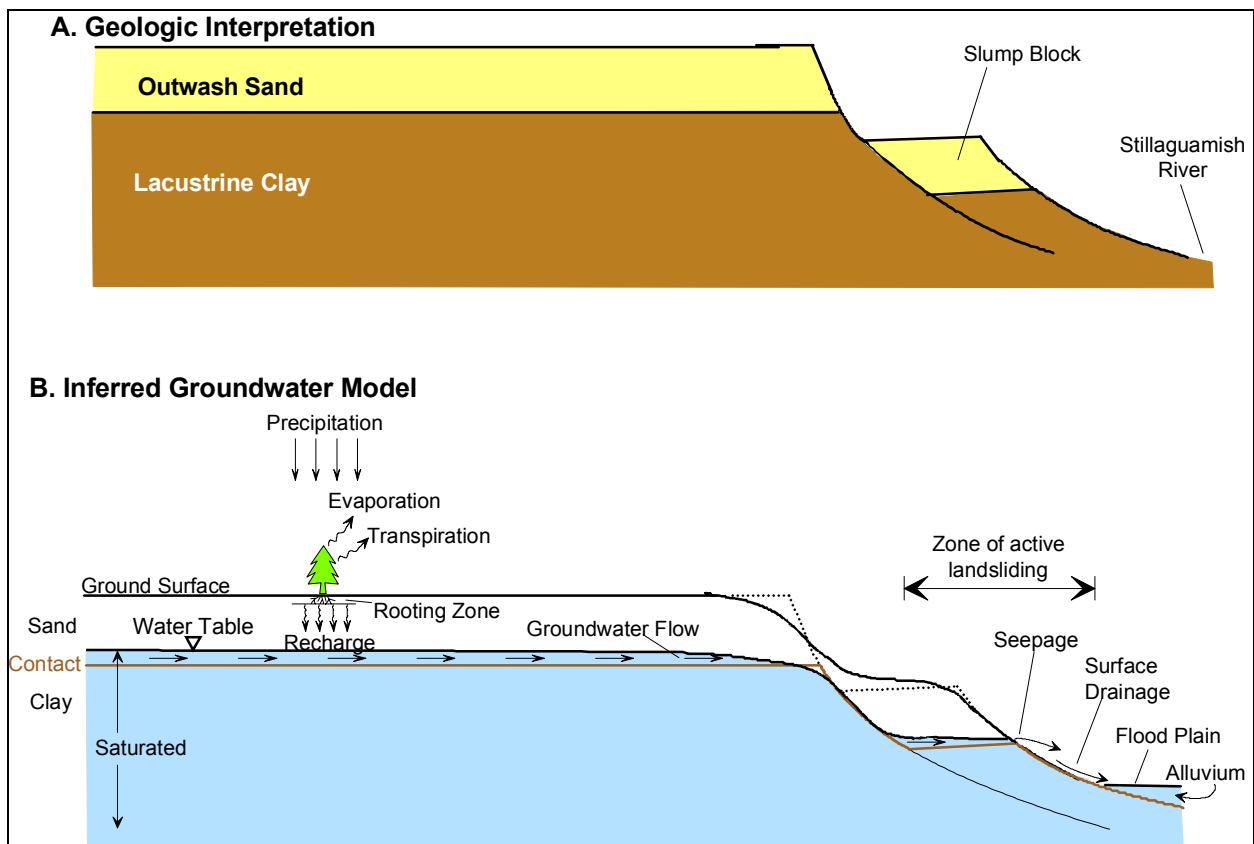


Figure 1.3. A conceptual model of groundwater flow to the Hazel landslide.

Historic Landslide Activity

The following chronology is based in part on preceding reports (Shannon and Associates, 1952; Thorsen, 1969; Benda et al., 1988; Wolff, 1988; DNR, in prep.) and in part on the tracings by Curtis (1988) and photographs shown in Figure 1.4. DNR (in prep) note in the Level 1 mass wasting analysis that 1937 photographs (archived with the Snohomish County Public Works Department) show the river making a tight bend at river mile 20 and that the Hazel landslide was active. Benda et al., (1988) estimate the landslide had encompassed about 10 acres by 1942, although the tracings made by Curtis (1988) indicate the landslide was relatively inactive at that time. The first detailed study of the landslide is that of Shannon and Associates (1952), prompted because of concerns about turbidity. They note:

“As a direct result of this slide condition, the turbidity of the North Fork Stillaguamish River below the slide area has increased considerably over the past twenty years. The increase in turbidity is due to two actions: (a) the erosion by the river of the clay exposed along its north bank and (b) the erosion of the clay by small spring fed streams within the slide area.”

At the time of their report, the active landslide had already extended about 1000 feet from the river's edge, delineated by a distinct scarp reaching 70 feet high in places (visible in the 1955 photographs) and coming within about 150 feet of Headache Creek. They describe the landslide in terms of large blocks that had moved downslope, carrying their forest cover intact. They also report that in December of 1951, a mud flow originating from one of the channels draining the slide partially dammed the Stillaguamish River.

The 1965 photograph indicates great activity within the landslide. A large portion of the slide mass is without vegetation and the headscarp is clearly visible. Note also the recent harvest of the Headache Creek Basin, which, based on a forest-type map for the site (Newman, 1982), was done in 1960. Also visible in the photograph is a rock revetment, constructed in 1962 (Thorsen, 1969), lining the eastern portion of the slide along the river's edge. In January of 1967 a large volume of material was shed from the slide, burying the revetment and forcing the river to a new channel several hundreds of feet to the south. The change in river course is clearly visible between the 1965 and 1970 photographs. This event involved a slip surface considerably above river level, with movement occurring as mud flows and translational slumps (Thorsen, 1969).

Debris from the 1967 event then served as a primary source of landslide-derived sediment over the next two decades. The 1978, 1984, and 1987 photographs show the channel gradually eroding through this deposit back toward the pre-1967 channel course. This debris also served to protect the base of the landslide from further bank erosion by the Stillaguamish River over that time. By 1978 the landslide is largely revegetated, but exposed scarps throughout this time indicate persistent smaller-scale movements.

On Thanksgiving Day of 1988 another failure from within the landslide again forced the river south from its former channel, indicating that the river had once again impinged upon the base of the landslide. Wolff (1988) reports river-bank sloughing, a “high (50+ feet), near-vertical riverbank” downstream of the Thanksgiving Day failure, and “new tension cracks and mini-terraces” appearing over much of the 1967 scar. These observations suggest that toe cutting by the river had reinitiated movement within the main body of the slide mass. The 1991 photograph, following a very wet winter with high flood flows, shows activity concentrated along the western, downstream edge of the landslide. Large chunks of an ancient slump block have failed, probably moving initially as slumps and evolving into mud flows. Debris from these failures has again forced the river to a new course. Note that harvest has occurred upslope of this area on Whitman Bench.

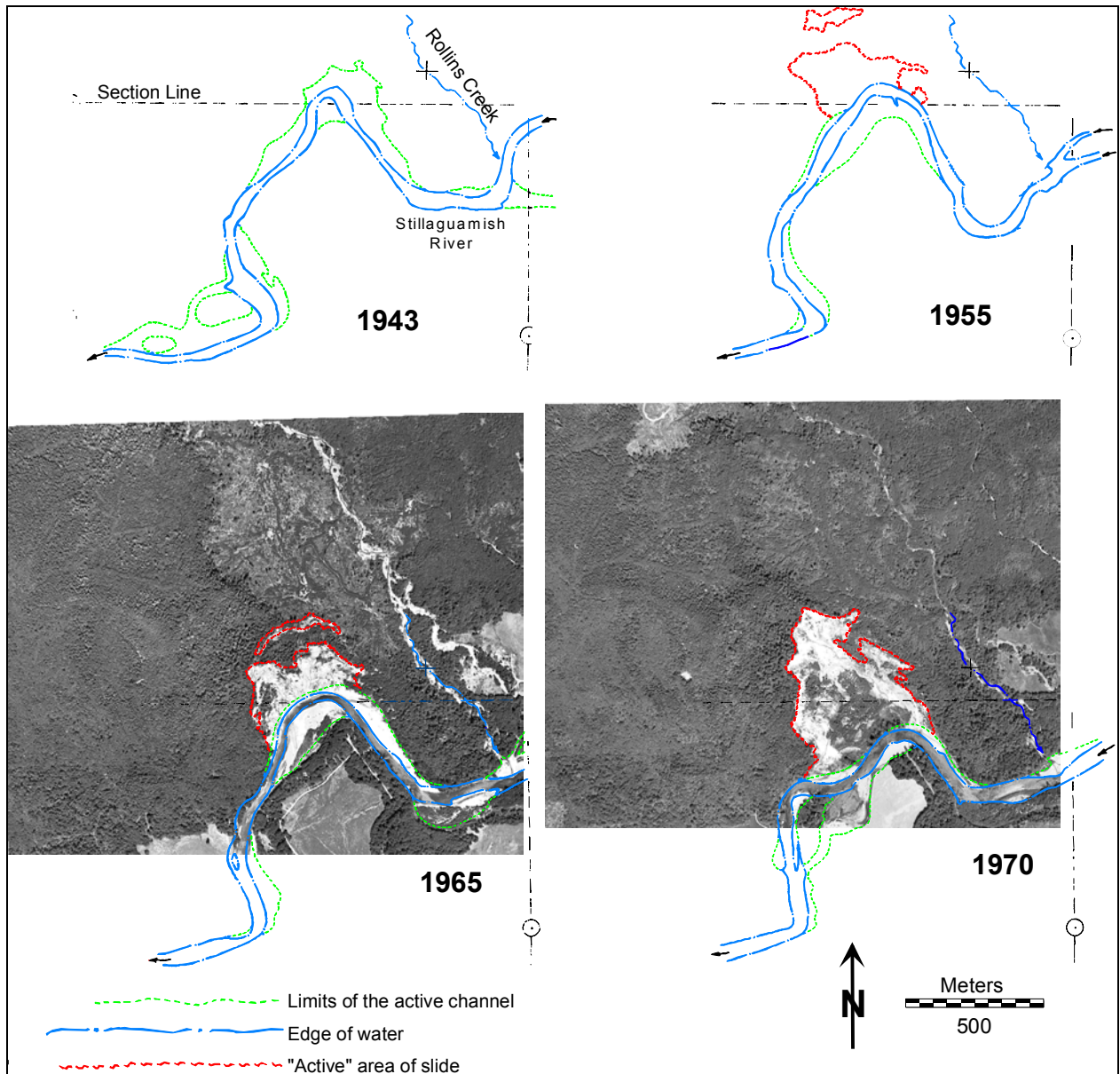


Figure 1. 4a. Historical activity on the Hazel slide. Tracings are from Curtis, 1988. Note harvest of the Headache Creek basin visible in the 1965 photograph. A large event in 1967, the scarp of which is seen clearly in the 1970 photograph, dramatically altered landslide topography and pushed the channel of the Stillaguamish southward. Debris from this event protected the landslide toe from bank erosion and was gradually eroded away over the course of the next 15 years.

By 1995 (because we have no photographs newer than 1991, the following remarks are based on field observations), following another very wet winter, the river was again impinging on the base of landslide slopes. Bank erosion was occurring along the entire length of the landslide toe, although upslope activity was concentrated in the zone of slumping visible in the 1991 photograph. The 1962 revetment had been almost completely exhumed and may act to protect the eastern portion of the slide from further toe erosion. Over the winter of 1996 slumping continued to eat headward into the ancient slump block on the western, downstream portion of the landslide. A large “blowout” also occurred along one of the channels draining the central portion of the landslide. It appears to involve a series of headward-eating slumps into the channel, although it is impossible to tell whether it was initiated by erosion of the channel or by slumping along the Stillaguamish.

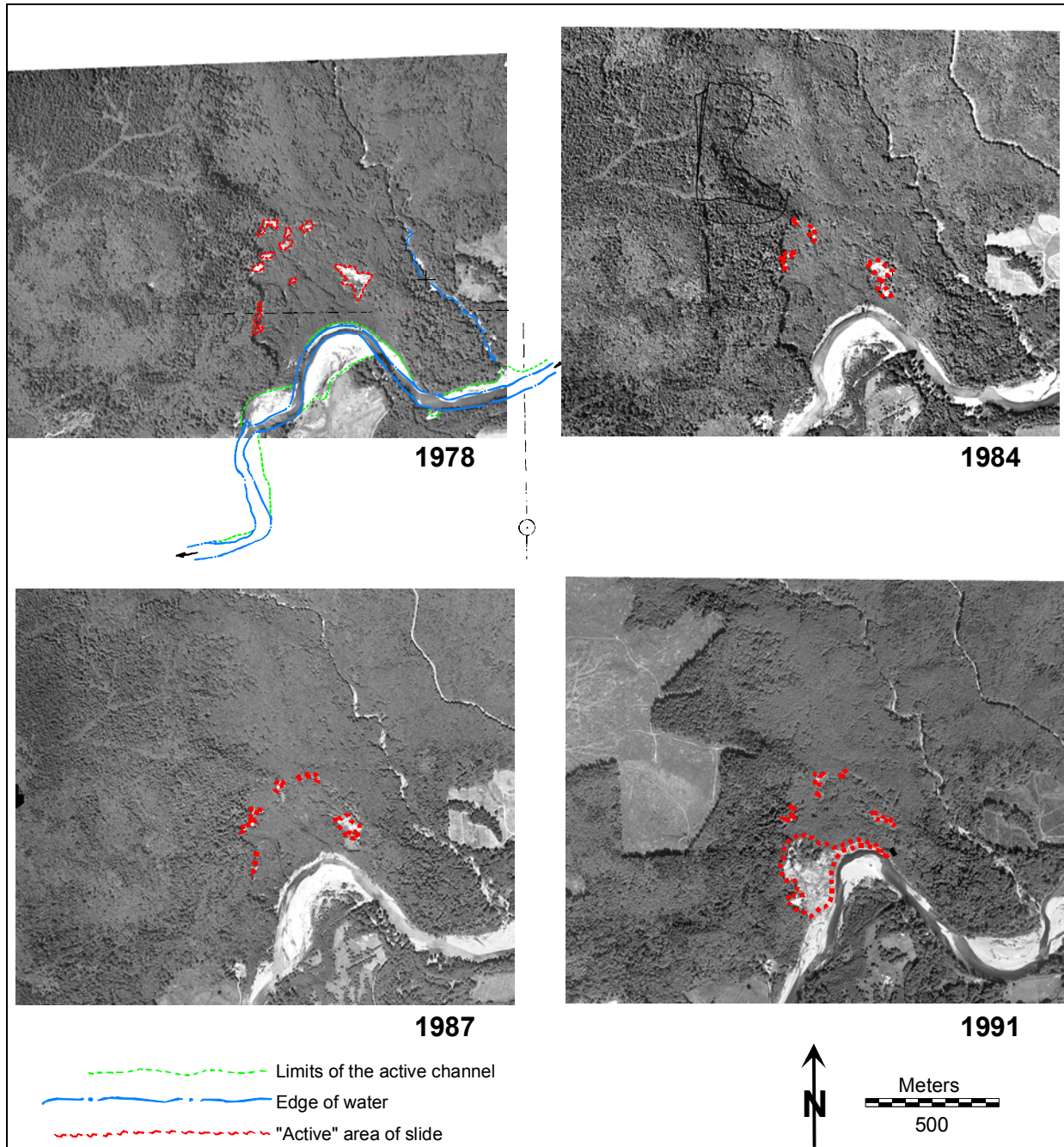


Figure 1.4b. Historical activity on the Hazel landslide. The landslide was relatively quiescent through the 1980s, with a few upslope zones of persistent activity. Activity along the toe resumed in 1988. We don't know if the harvest visible on the Whitman Bench in the 1991 photograph preceded or post dated the activity along the toe.

Tension cracks both up- and down-slope of headscarps lining the landslide continue to form and expand within the same zones of activity evident in the 1978, 1984, and 1987 photographs.

These observations yield two important points: 1) landslides that dump large volumes of material directly into the Stillaguamish River, such as those of 1967, 1988, and again during the 1990s, occur only when the river is impinging directly on the landslide toe, and 2) timber harvest in potential recharge areas preceded the 1967 and 1990 landslide activity. Whether these correlations are purely coincidental or represent true relations of cause and effect is debatable. We attempt to clarify the relationships in the remaining sections of this report.

References

- Benda, L., G. W. Thorsen, and S. Bernath, 1988, *Report of the I.D. team investigation of the Hazel Landslide on the North Fork of the Stillaguamish River* (F.P.A. 19-09420), Report to the Department of Natural Resources, Northwest Region, Sedro Woolley, 13 p. plus 2 figures*
- Booth, D. B., 1989, *Surficial Geologic Map of the Granite Falls 15-Minute Quadrangle, Snohomish County, Washington*, U.S. Geological Survey Miscellaneous Investigations Series, Map I-1852
- Collins, B., T. Beechie, L. E. Benda, P. Kennard, C. Veldhuisen, V. Anderson, and D. R. Berge, 1994, *Watershed Assessment and Salmonid Habitat Restoration Strategy for Deer Creek, North Cascades of Washington*, Report to Washington State Department of Ecology and Stillaguamish Tribe of Indians: 10,000-Years Institute, Seattle, WA, 232 p.
- Curtis, T., 1988. Mylar overlays showing the historical movements of the Stillaguamish River in the vicinity of the “Hazel Slide” for the years 1943, 1955, 1965, 1970, and 1978, Department of Natural Resources, Northwest Region, Sedro Woolley*
- DNR, in prep, Level 1 Hazel Watershed Analysis, Washington State, Watershed Analysis Report, Washington Department of Natural Resources, Northwest Region, Sedro Woolley*
- Freeze, R. A., and J. A. Cherry, 1979. *Groundwater*, Prentice-Hall Inc.: 604 p.
- Kennard, P., and G. Pess, 1994, *Forest Management and Stream Degradation in Montague Basin – A Watershed Assessment*, unpublished report, Tulalip Tribes Environmental Department, Marysville, WA, 44 p.
- Newman, 1982. Hand-drawn stand-type map*
- Shannon, W. D., and Associates, 1952, *Report on slide on North Fork Stillaguamish River near Hazel, Washington, to the State of Washington Departments of Game and Fisheries*, 18 pp. plus appendix by H. Coombs, 8 plates*
- Tabor, R. W., D. B. Booth, J. A. Vance, and A. B. Ford, 1988, *Geologic Map of the Sauk river 30- by 60-Minute Quadrangle, Washington*, U. S. Geological Survey Open File Report 88-692, 50 p., 1 map sheet
- Thorsen, G. W., 1989, Landslide provinces in Washington, in R. W. Galster (ed), *Engineering Geology in Washington*, Volume 1, Bulletin 78, Washington Division of Geology and Earth Resources, Department of Natural Resources, p. 71-89.
- Washington Forest Practices Board, 1995. *Board Manual: Standard Methodology for Conducting Watershed Analysis*, Version 3.0: Olympia
- Wolff, N., M. Nystrom, and S. Bernath, 1989, *The effects of partial forest-stand removal on the availability of water for groundwater recharge*, report submitted to H. Villager, Northwest Regional Manager, Department of Natural Resources, Northwest Region, Sedro Woolley, 14 pp.*
- Wolff, N., 1988. Hazel Slide / Thanksgiving Day 1988 Failure, handwritten note on file, Department of Natural Resources, Northwest Region, Sedro Woolley*

* on file at Department of Natural Resources, Northwest Region, Sedro Woolley

Simulation of groundwater recharge at Hazel in relation to vegetation cover

Joan Sias

Logging has been identified as a possible factor in increased landslide activity at Hazel, due to the physical relationships between vegetation cover, evapotranspiration, and groundwater pore pressures. Groundwater pore pressures depend on aquifer characteristics and patterns of recharge over time and space. Recharge, in turn, is equal to gross precipitation less evapotranspiration, less overland flow. Evapotranspiration is the sum of direct evaporation from a wet surface (*e.g.* vegetation, litter, bare soil) and transpiration by a dry canopy. Tall vegetation and short vegetation have different physical and biological characteristics that can lead to substantially different rates of evapotranspiration and, therefore, recharge. For well-drained locations, recharge can be equated with water yield (overland flow is zero); these two terms will be used interchangeably hereafter.

The purpose of the work described in this paper was to estimate the change in groundwater recharge for well-drained sites on the drainage area to the Hazel landslide, before and soon after clearcutting of a stand of evergreen trees. Empirical paired-catchment studies provide some indication of the magnitude of change in recharge that could be expected at Hazel. Hazel has a mean annual rainfall estimated to be between 1500 to 2000 mm (Wolff *et al.*, 1989). Above a mean annual precipitation of 1200 mm, the change in water yield is about 45 mm +/- 20 mm when 10 percent of a humid forested basins basin area is clearcut (Bosch and Hewlett, 1982). The large uncertainty in this statistic points to the importance of site-specific factors, as noted also by Stednick (1996) and Wolff *et al.* (1989).

Wolff *et al.* (1989) identified the major issues pertaining to the hydrological effect of a proposed selective partial cut within the drainage basin to the Hazel landslide. In this report we evaluate the effect of clearcut logging at Hazel. We attempt to account for the site-specific factor of local climate. Other site specific factors are treated as model parameters estimated on the basis of a literature survey. Because the valuable timber is mainly situated on well-drained soils at Hazel, the estimation of recharge for a forested and deforested scenario is cast as a problem of estimation of evapotranspiration. The desire to perform a transient analysis in particular necessitated that evapotranspiration be estimated by a time series simulation. For this purpose we selected the physically based Penman-Monteith equation (Monteith, 1965).

The Penman-Monteith equation was selected because of its strong physical basis. Since it is a physical model rather than a regression model, in theory the parameters can be determined directly, prior to application of the model. To the extent that parameters are accurately determined, the model should be able to accurately predict evapotranspiration at a site. A great deal of experience with the Penman-Monteith equation shows that this equation does indeed accurately predict evapotranspiration from wet and dry canopies if the parameters are well determined (see *e.g.*, McNaughton and Black, 1973; Kelliher, *et al.*, 1986; Rutter *et al.*, 1971).

Overview of Approach and Major results

The model was used to simulate soil moisture content, transpiration, and interception loss at a point for two scenarios:

1. forest, well-drained
2. clearcut, well-drained with newly established deciduous vegetation cover

We have no actual measurements at Hazel from which we can estimate vegetation parameters directly. Therefore, for each of the two vegetation covers, we estimated on the basis of published reports a probable range of values for each vegetation parameter required in the model. We formed three recharge cases - high, low, and intermediate - for each vegetation scenario by setting parameters to their lower bound, intermediate, and upper bound values. For each case, the vegetation was treated as having constant attributes (either forested or clearcut) over the period of simulation. Climate was assumed invariant with changes in vegetation. Evapotranspiration (and by difference, recharge) was simulated for each case.

Uncertainty in the values to assign to the vegetation parameters in the model translate to uncertainty in the calculated recharge. The simulation results for these scenarios constrain the range for forest and clearcut recharge rates for a well-drained patch of land at the Hazel landslide.

Meteorological forcing data at Hazel were inferred from long-term climate observations at Darrington, WA, the nearest location for which a lengthy meteorological record was available. Examination of average water balance components over the 61-year simulation period (1935-1994) shows the following:

- The uncertainty range for average annual recharge is small for the clearcut (about 1200 to 1400 mm), but is large for the forest (about 500 to 900 mm).
- The uncertainty in forest evapotranspiration is largely due to differences in the magnitude of winter evapotranspiration losses. Summer evapotranspiration loss changes relatively little among the high, medium, and low recharge cases.
- The change in average annual recharge after clearcutting could be as low as about 300 mm or as large as about 900 mm.
- The most conservative estimate for forest evapotranspiration is probably overly conservative, and the corresponding recharge estimate somewhat high. It is likely that forest average annual recharge is closer to 500 mm than 900 mm. Likewise, the lower estimate of 300 mm for average annual change in recharge due to clearcutting is probably overly conservative.

In concluding this report, we identify the kinds of data and further analysis that could enable this uncertainty range to be greatly reduced.

Model description

The evapotranspiration model simulates interception loss, soil moisture status, stomatal resistance, and transpiration for a forest and clearcut, assuming well-drained soil. For well-drained soils recharge is simply the difference between gross precipitation and simulated evapotranspiration; there are no inputs or losses due to overland or lateral subsurface flow. The model operates on a six-hour time step, since a longer time step would be inappropriate for the Penman-Monteith calculation (McNaughton and Black, 1973).

The site conditions are such that it was considered unnecessary to model the following: direct runoff due to saturation and infiltration excess overland flow, snow accumulation and melt, direct evaporation from other than the vegetation canopy, and time-dependent redistribution of moisture within the root zone. We assumed that additions to groundwater occurred with no attenuation of moisture draining from the root zone, but we do recognize that this could have an important effect in a transient analysis.

We do not simulate evapotranspiration losses on the landslide itself, where the groundwater table intersects the surface and seepage is occurring. In general, vegetation-mediated evapotranspiration loss on the exposed lacustrine deposits will have a different hydrologic effect than evapotranspiration loss mediated by coniferous trees rooted in well-drained soil above the active landslide. Some portions of the landslide support stands of alder whose roots have access to the groundwater. Over the summer growing season, these stands of alder may actually have a net effect of discharging the reservoir. In the groundwater simulations, we treat the exposed lacustrine deposits on the landslide as non-vegetated. If we were to include this vegetation, it is conceivable that there could be an effect on average end-of-summer season groundwater level over a larger portion of the drainage area.

We use a model similar to that described by Kelliher *et al.* (1986). These authors applied the Penman-Monteith equation with a modified Rutter interception model (Rutter *et al.*, 1971) and a soil moisture accounting scheme to a two-layered representation of a 31-year old thinned Douglas fir stand on Eastern Vancouver Island. The authors use regression equations to estimate stomatal resistance as a function of vapor pressure deficit and soil moisture tension. With this model Kelliher *et al.* (1986) found good agreement between the simulated and measured growing season evapotranspiration. We depart in certain ways, mainly in that we assume a single-layered closed canopy (Whitehead and Kelliher, 1991). The model parameters are listed in Table I. The model is described in some detail in Appendix I, as is the estimation of these parameters.

The model parameter limits for the forested case were estimated mainly on the basis of summer season measurements made on Douglas fir stands in Eastern Vancouver Island (*i.e.* stomatal resistance function), and in the rainfall-dominated lower elevation Oregon Cascades. We assume that the parameters for a Douglas fir stand would be similar enough to other species occurring at Hazel, relative to model sensitivity to these parameters, to warrant neglect of possible species differences. The clearcut parameters were estimated from data or generalizations about short herbaceous vegetation.

Table I. A: Model parameters

r_a	aerodynamic resistance
r_s -min	minimum stomatal resistance
LAI	leaf area index
FTHRU	fraction throughfall plus stemflow
RZ-max	maximum root zone storage (storage at field capacity)

Table I. B: Upper and lower parameter bounds, intermediate value

Parameter	Units	Evergreen Forest			Clearcut	
		lower	middle	upper	lower	upper
r_a	s/cm	0.1	0.07	0.04	0.3	1.2
r_s -min	s/cm	2.5	2.5	2.5	2.0	1.5
LAI	m ² /m ²	5	7	10	0.75	1.50
FTHRU	dimensionless	0.8	0.70	0.65	0.90	0.80
RZ-max	mm	200	250	300	100	150

Meteorological data

The hydrologic model requires the following meteorological variables at a six-hourly time step: precipitation, air temperature, net radiation, and vapor pressure deficit. As we have no measurements of these variables at Hazel, they must be inferred from data at nearby climate stations. The nearest long term climate station is at Darrington, WA, 11 miles to the east of Hazel. The available electronic data coverage for this National Weather Service cooperator station is for the period October 1931 to September 1994. This meteorological data set consists of 24-hour precipitation totals and daily minimum and maximum air temperature. Daily

precipitation and temperature extremes are estimated for Hazel directly from these observations at Darrington. Six-hourly air temperature, net radiation and vapor pressure deficit are inferred using the algorithms described in Appendix II.

In orographic settings, precipitation for individual storms and on an annual basis can vary strongly over space. The average annual precipitation at Darrington (1931-1993) is 89.5 inches. Wolff *et al.* (1989) estimate that average annual precipitation at Hazel is between 60 to 80 inches. We assume that the 24-hour precipitation amounts at Hazel are equal to precipitation at Darrington times the factor 7/9.

Temperature variation over space is more predictable than precipitation; it is common to assume that at constant elevation, temperature is conserved over horizontal distances of tens of kilometers. The weather station at Darrington (500 ft above sea level) is situated at approximately the median elevation for Hazel. Therefore it was unnecessary to make any adjustment to the Darrington air temperature data for elevation differences between the two sites. It is common to assume that air temperature varies with elevation at the rate of about 0.1 °C per 500 ft (Linsley *et al.*, 1975). The elevation range at Hazel (300 to 800 ft above sea level) is small enough that the variation of temperature with elevation can be ignored.

We did not attempt to simulate snow accumulation and ablation. All precipitation is assumed to occur as rainfall. It is highly likely that snowfall does occur at Hazel; however snow cover is short-lived at this low elevation. The mischaracterization of the physical form of precipitation could have some effect on the transient groundwater simulation. The simulated average annual water balance would not be significantly affected by the inclusion of a snowmelt model, and therefore the steady-state groundwater simulations are not sensitive to this omission.

The physical setting of the climate station is relevant to the interpretation of the model results (see Discussion). The climate data at Darrington is collected in a park-like setting within the town of Darrington. The forest edge is within 1 to 2 miles in each compass direction except to the west. To the west, forest cover is patchy. Wind speed is measured in summer only; a typical summer's day wind speed is 3 m/s. The predominant wind direction is up-valley, into the Cascades (out of the south). At Hazel the upwind terrain is also patchy, and fetch is limited.

Appendix II describes the methods used to infer 6-hourly precipitation, air temperature, vapor pressure deficit, net radiation. The ambient atmospheric conditions could depend on vegetation cover. However, it is not feasible to model vegetation-atmosphere interactions, and therefore it was assumed that precipitation, air temperature, and therefore vapor pressure deficit are the same over both vegetation endpoints.

Results

A. Average annual water balance.

Annual water balance components were calculated for each simulation on an October-September water year basis. The simulation period, October 1931 to September 1994, corresponds to the length of the available meteorological data for Darrington. The appropriate soil moisture value at the start of the simulation is unknown. It was necessary to assume an initial value. To avoid any

influence of assumed initial soil moisture condition on model output, we disregarded results from the first three years of the simulation (water years 1932-1934).

The simulated water balance components for the 60 year period 1935 to 1994 are shown in Figure 1. Mean annual precipitation over this period is 1685 mm. We use ‘low’ and ‘high’ recharge cases to represent the results obtained for all parameters set to their ‘upper’ bound and ‘lower’ bound, respectively, where ‘upper’ and ‘lower’ is defined in reference to evapotranspiration. The upper parameter bound, for example, is the limit which corresponds to high evapotranspiration and low recharge. Most parameters are defined such that the lower bound is numerically smaller than the upper bound. An exception to this is FTHRU.

The results in Figure 1 are summarized as follows:

1. Forest average annual evapotranspiration ranges from 763 to 1174 mm. The corresponding recharge values are 923 and 512 mm, respectively.
2. Forest annual interception losses exceed summer transpiration losses for the forest, but are

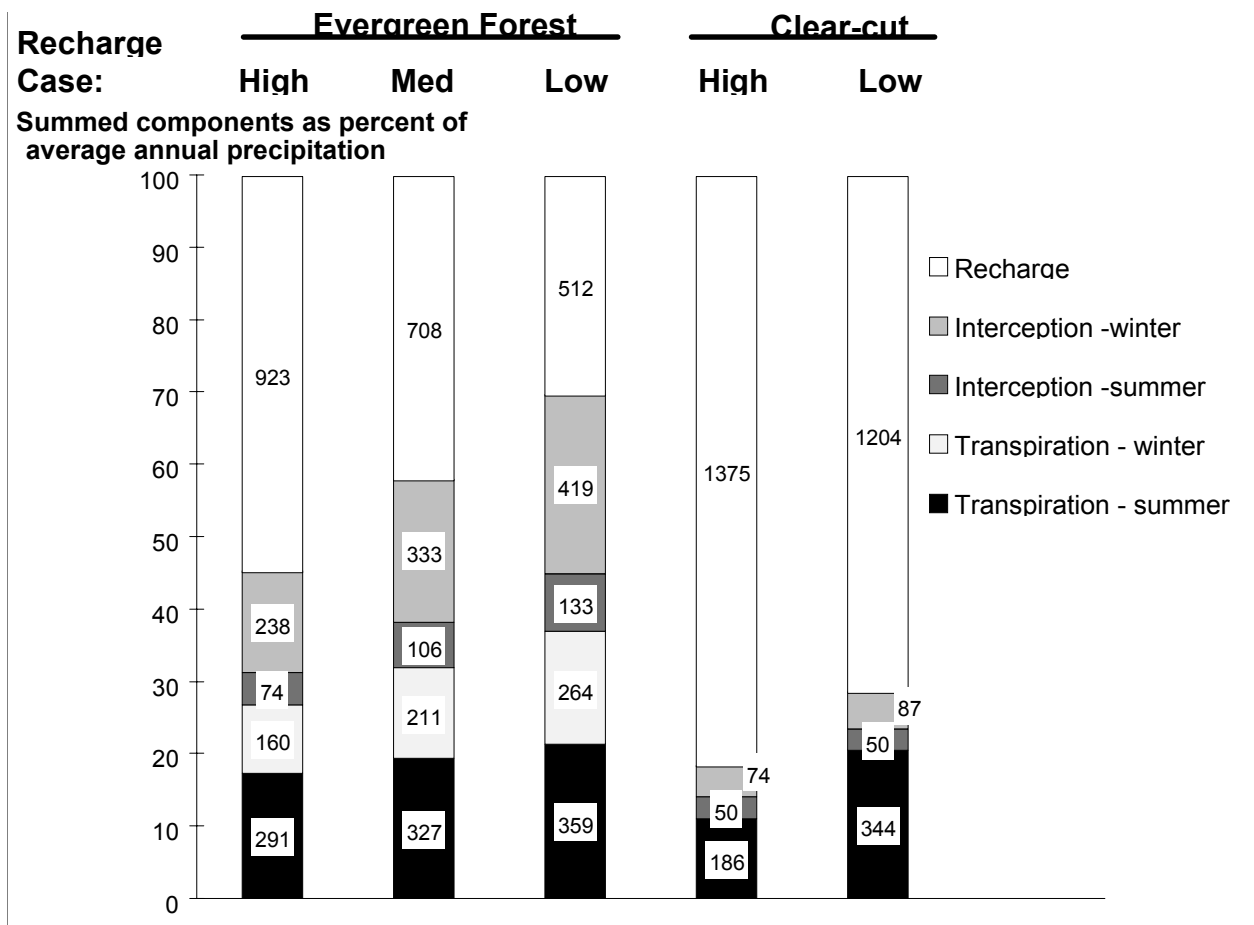


Figure 1. Simulated water balance components for forest and clearcut scenarios. The sum of the water balance components is equal to 100 percent of average annual evapotranspiration (1686 mm). The magnitude of each component (average annual depth in mm per year) is given in the highlighted boxes.

minimal for the clearcut. The remaining component of annual evapotranspiration is winter transpiration loss. This accounts for about 15% of forest annual evapotranspiration.

3. Clearcut evapotranspiration is not zero, because we assumed rapid revegetation with a short deciduous cover. Compared to the forest, the clearcut evapotranspiration seems to be quite predictable. The uncertainty range for clearcut evapotranspiration is 310 to 481 mm/yr. Average recharge ranges from 1204 to 1375 mm for the clearcut scenarios.

Table II lists the average annual recharge for each scenario. The difference between the forest low recharge case and the clearcut high recharge case forms the conservative estimate for change in recharge due to clearcutting. The medium and low estimates for change in recharge are formed similarly.

Table II. Recharge scenarios: change in recharge due to clearcutting

Scenario	Recharge (mm)		
CLEARCUT	LOW 1204	MED. 1343	HIGH 1375
FOREST	HIGH 923	MED. 708	LOW 512
		<u>DIFFERENCE:</u>	
CHANGE IN RECHARGE DUE TO CLEARCUTTING:	281	665	863

B. Time series of soil moisture

In Figure 2 we show a partial time series of simulated recharge and soil moisture for the forest and clearcut medium recharge cases. Soil moisture here means that accessible to plant roots. Moisture in the root zone is depleted by transpiration and replenished by throughfall. Recharge can only occur when soil moisture content has reached the maximum attainable value (RZ-max in Table I.). RZ-max was assumed to be 250 mm for the forest and 125 mm for the clearcut for the two simulations shown. Note the shift of +125 mm for the clearcut soil moisture time series (see legend to Figure 2). Compared to the forest simulation, soil moisture for the clearcut less often falls below RZ-max (125 mm, but shown as 250 mm on the axis). These patterns of soil moisture lead to higher recharge in the clearcut throughout most of the year, and earlier timing of the first large recharge event in the fall. During the wettest periods, the five-day recharge peaks are higher for the clearcut. This is mainly because of lower interception loss in the clearcut.

C. Sensitivity analysis

In order to understand which parameters explain the large range in forest evapotranspiration, a simple sensitivity analysis was performed. Figure 3 shows, for the forested simulation, the effect of independently changing parameters from the intermediate value to either the lower bound or

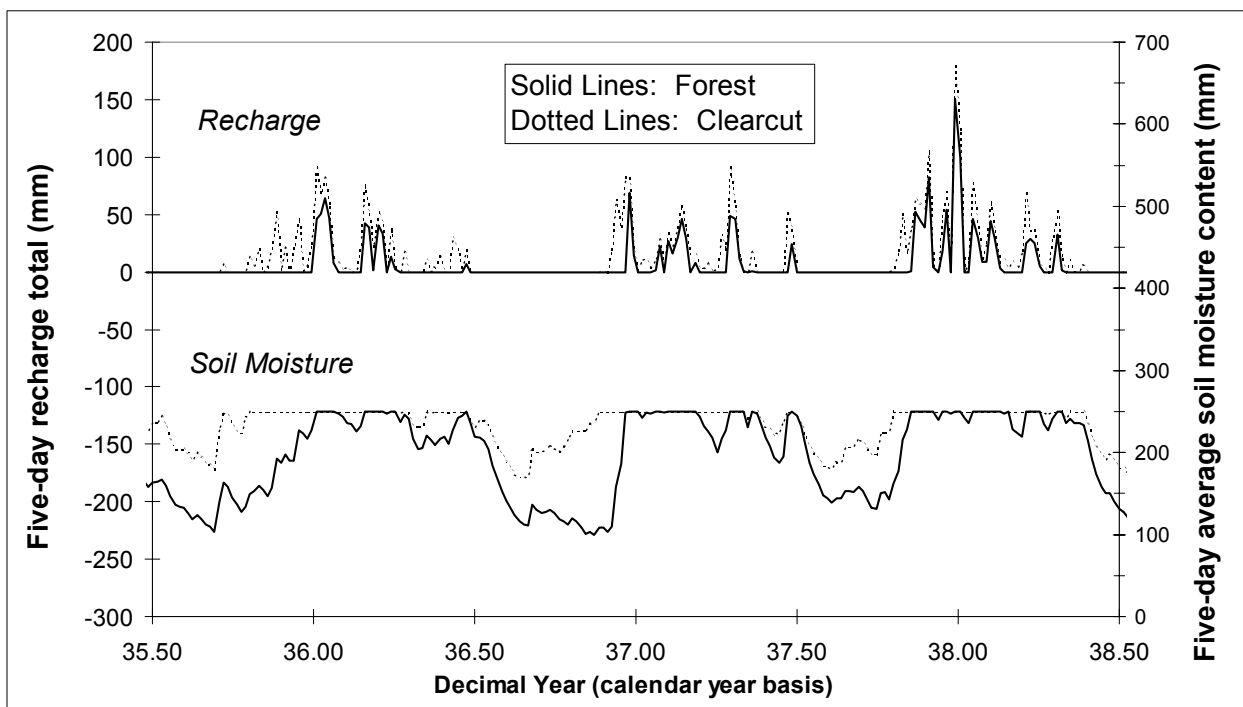


Figure 2. Time series of recharge and soil moisture for the forest and clearcut scenarios (medium recharge cases). Moisture capacity is 250 mm and 125 mm for the forest and clearcut, respectively. For convenience both are shown as at field capacity at 250 mm on the axis. Forest soil moisture can vary between 0 and 250 mm; as shown, clearcut soil moisture can vary between 125 and 250 mm.

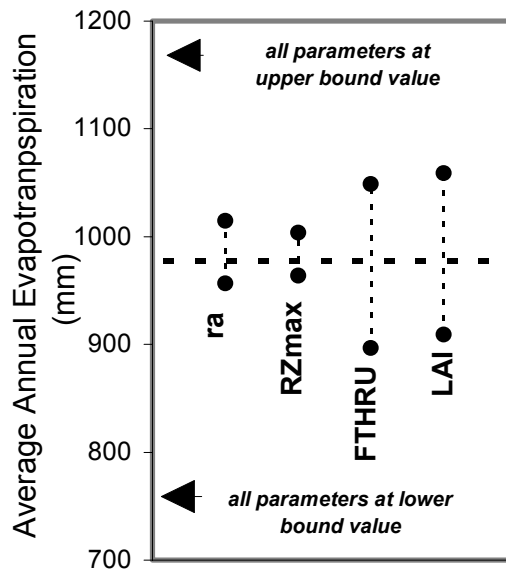


Figure 3. Forest evapotranspiration is increased or decreased from 978 mm when one parameter is changed from its intermediate to its upper or lower bound, with all other parameters at the intermediate value. 987 mm is the result for the intermediate recharge case. Parameters are defined in Table I.

the upper bound, while holding all other parameters at the intermediate value. Minimum stomatal resistance is not shown, since it was held constant for each vegetation cover. The ranges shown for FTHRU and LAI, the most sensitive parameters, amount to 37 percent of the difference in average annual evapotranspiration between the high and low recharge cases. Because FTHRU and LAI affect the water balance in different ways, their effects are additive: Changing both parameters accounts for about 70 percent of the difference in the two limits.

Figure 4 shows the variation in the components of evapotranspiration for different values of throughfall fraction (FTHRU) and leaf area index (LAI). Direct evaporation increases by 650 mm as throughfall fraction goes from 0.8 to 0.0, and total evapotranspiration by 450 mm. Over the range we considered appropriate to a closed evergreen canopy at Hazel, 0.8 to 0.65, the interception rate almost doubles from 316 to 600 mm/yr, whereas total evapotranspiration increases by about 150 mm. The smaller change in evapotranspiration is due to a partially compensating change in transpiration loss. Transpiration loss increases as interception fraction decreases because, on average, less moisture remains on the canopy upon cessation of rainfall. Consequently, the canopy dries a little faster after storms, and the interval for transpiration is slightly longer. Direct evaporation does not go to 100% of storm precipitation at a throughfall fraction of zero. This is because, as described in Appendix I, the canopy interception model allows for drainage (additional throughfall) from the canopy when the rainfall rate exceeds the evaporation rate, as frequently happens in the winter.

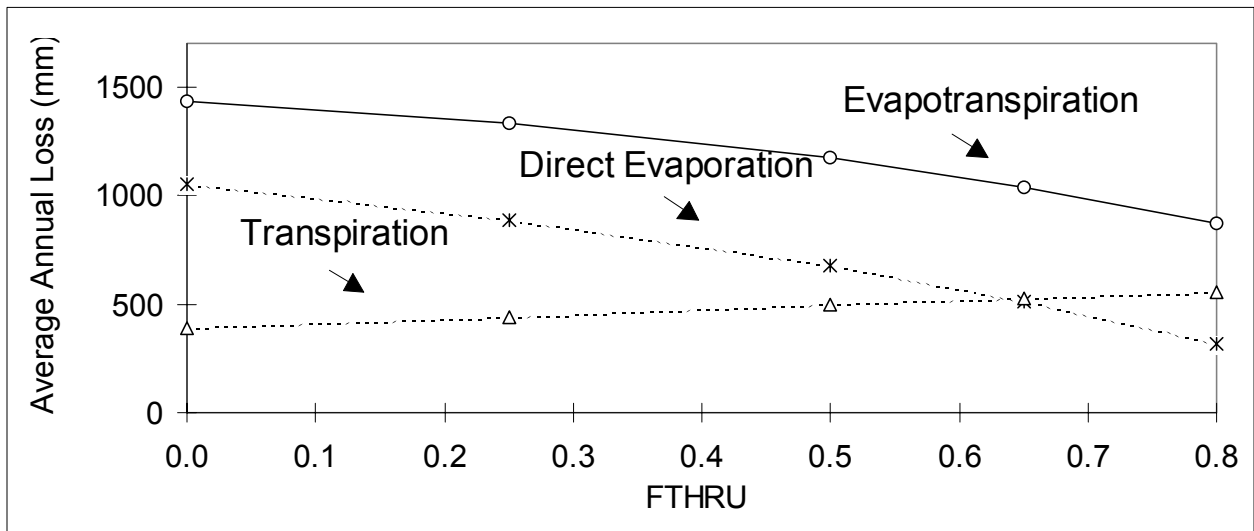


Figure 4. Change in water balance components with change in FTHRU (throughfall fraction) for the forest scenario, medium recharge case.

The relationships shown in Figure 4 are not sensitive to the canopy storage capacity. This is because for this climate (low intensity, long duration storms), most direct evaporation occurs *during* storms, whereas canopy storage capacity only affects the amount of direct evaporation that occurs from a drying canopy *after* rainfall ceases

Values for FTHRU as low as 0.4 could be reasonable for mature Douglas fir forest (> 70 years old), but then only under poor growing conditions (Giles *et al.*, 1985) and strong advection. Lower values, corresponding to canopy gap fraction plus stemflow, might be a reasonable assumption where rainfall occurs mainly as snow (*e.g.*, Wigmosta *et al.*, 1994), or when the model includes an explicit drainage term (*e.g.*, Rutter *et al.*, 1971).

Discussion

As simulated, clearcut evapotranspiration is likely to be only slightly less than summer evapotranspiration for the forest. The difference in forest and clearcut evapotranspiration seems to be due mainly to differences in winter fluxes for the forested case.

The approach of estimating parameters from literature data leads to a large uncertainty in the simulation results for the forest. Most of the variability in the forest evapotranspiration results is due to the parameters LAI and FTHRU (Figure 3). LAI determines the transpiration surface area and the interception store capacity. We found that most of the interception loss is occurring during storms, and that interception loss is therefore quite insensitive to the interception store capacity. LAI then is important mainly for summer and winter transpiration loss. FTHRU is important mainly for winter evaporation loss.

In retrospect, we were probably overly conservative in choosing 5.0 for the lower bound value for LAI. The upper bound value is well-supported as a typical value for old growth forest. If this is taken into consideration, then throughfall fraction is a stronger determinant of the annual water balance than is LAI. Effort to reduce the uncertainty range then should focus first on FTHRU. We note that LAI could be estimated quite easily, to more or less accuracy, by application of regression equations developed for Oregon stands (*e.g.* Gholz, 1982). These regressions equations relate LAI to tree species and diameter-at-breast-height. Field estimation of throughfall fraction is more expensive and time consuming, since storms of various magnitudes should be sampled.

The winter transpiration losses - more than 50 percent of summer losses - seem quite high, but we have not found any published values for winter transpiration rates that might be relevant to Hazel. Winter transpiration losses range from about 10 percent (169 mm) to 18 percent (264 mm) of annual precipitation for the three forest scenarios. The mild climate at the low elevation of Hazel, however, may well support substantial winter transpiration. Reed and Waring (1974) have noted that Douglas firs (and therefore presumably other species as well) can continue to transpire until air temperature falls below 2 °C. This threshold happens to correspond to the average monthly air temperature at Darrington in January. It is known also that significant carbon fixation can occur during the dormant season if daytime temperatures are mild enough (Emmingham and Waring, 1977), and therefore transpiration must also be occurring.

Most likely the model oversimplifies the factors affecting winter transpiration rates, and is overestimating winter rates by some unknown amount. For example, Emmingham and Waring (1977) found that carbon fixation was reduced following cold nights. It could be that stomata are also similarly sensitive.

A remaining question is whether the meteorological data collected at Darrington is representative of conditions over the forest at Hazel. One problem is that we are using data collected over a clearing to estimate fluxes over a forest. Pearce *et al.* (1980a) found that this procedure led to a 30 percent overestimate of forest evapotranspiration for a stand in New Zealand. This may not be such a major issue at Hazel. The upwind geography at Hazel would seem to be sufficiently short (less than several kilometers), so that conditions over an upwind clearing (or at Darrington) may not diverge tremendously from those over the forest at Hazel.

A related concern is whether the during-storm vapor pressure deficit is accurately estimated. Rutter *et al.* (1977) found that over a forest, potential evaporation during rainy hours was about half that during non-rainy hours. Presumably this is due to negative feedback of during-storm canopy evaporation onto vapor pressure deficit (McNaughton and Jarvis, 1983). The algorithm we used to estimate vapor pressure deficit (Appendix II) does not directly deal with negative feedback, it does not differentiate rain/non-rain periods and it has been validated only in summer.

The recharge cases for each cover were formed by setting all parameters to their upper or their lower or their intermediate value (Table I). To form the limiting cases in this way is reasonable. A canopy of high leaf area index will tend to intercept more rainfall than a canopy of low leaf area index, and will tend to be taller also. Thus the high leaf area index canopy will tend to have a lower value for the parameter FTHRU; it will also tend to be a rougher surface by virtue of its

greater height, and therefore will have a higher aerodynamic resistance. Summer transpiration varies relatively little for the clearcut and forest scenarios.

Unfortunately, we have not identified any appropriate rainfall-runoff data in the Cascade foothills area of Puget Sound against which to compare the forest evapotranspiration estimates for Hazel. However, the following observations support certain aspects of the model results:

1. Using a weighing lysimeter, Fritschen *et al.* (1977) measured summer/fall evapotranspiration for a single Douglas fir tree in the Cedar River watershed, in western Washington, over three years to be about 500 mm. The elevation at this site was 702 feet. The results were 465 mm for April-Dec., 1972, 357 mm for June-Nov., 1973, and 517 mm for April-Oct., 1974. The simulated summer evapotranspiration (April-September) for the three forest scenarios range from 365 to 492 mm. The simulated values would be somewhat higher if early fall evapotranspiration were included in the totals. Nevertheless, the simulated and reported values seem to compare reasonably well.
2. There is little data from which to validate winter interception and transpiration losses. Measurements of transpiration have rarely been made in winter, and winter evapotranspiration losses in the PNW are most likely elevation dependent. Therefore the interception loss we estimate at Hazel should only be compared to data for a site with similar vegetation and climate. We are aware of only one empirical estimate that might be comparable to findings at Hazel: Pearce *et al.* (1980b) measured an annual interception loss of 560 mm for a coastal northwestern New Zealand mixed evergreen forest. Mean annual precipitation over the study period was 2075 mm. The study area was located at a similar, but southerly, latitude as Hazel. This result shows that high interception losses do occur in forested areas with high rainfall and moderate climate.
3. Table III lists all paired watershed studies which have been conducted in the Pacific Northwest, and for which the percent area cleared in one year was close to 100 percent (Stednick, 1996). All four studies listed were conducted in Oregon. The forest types represented include Douglas fir and Douglas fir-hemlock forests. The range of estimates of forest evapotranspiration for the three recharge scenarios (763, 978, and 1174 mm) look reasonable compared to the values shown in Table III. (We discuss above the issue that the lower bound value for forest LAI is probably too low, and that 763 mm is an overly conservative estimate for forest evapotranspiration)
4. The data in Table III seem to confirm the several hundred millimeters of evapotranspiration predicted for the clearcut. For a paired watershed study, water yield increase is equal to the difference between forest and clearcut evapotranspiration. For four out of five studies, water yield increase is less than average annual evapotranspiration by about 200 to 500 millimeters.

Table III. Summary of Paired Watershed Studies in Oregon ^a

Area (ha)	Elev. (m)	Area cut ^b (%)	Soils	Mean Annual Precipitation (mm)	Mean Annual ET (mm) ^c	Water Yield Increase (mm)
70 ^d	312	82	Loam	2480	595	615
96 ^e	700	100	Volcanic	2390	1010	462
13 ^f	900	100	Volcanic	2150	860	425
50 ^g	900	100	Gravel loam	1230	600	360
9 ^h	900	100	Volcanic	2330	680	460

^a A selective summary of data compiled by Stednick (1996)

^b The clearcuts were all completed within one year to the level indicated

^c Annual evapotranspiration (ET) was obtained by subtracting mean annual streamflow from mean annual precipitation for each basin

^d Needle Branch, OR; Harris (1973,1977), Harr(1976)

^e H.J. Andrews, OR, Watershed #1; Rothacher (1970)

^f H.J. Andrews, OR, Watershed #6; Harr (1976), Harr *et al.* (1979, 1982)

^g Coyote Creek, OR, Watershed #3; Harr (1976), Harr *et al.* (1979)

^h H.J. Andrews, OR, Watershed #10; Harr (1976), Harr *et al.* (1979)

Conclusions

The major findings are as follows.

1. The change in recharge due to clearcutting is estimated to be, most conservatively, on the order of 300 mm. This estimate is based on an overly conservative assumption about leaf area index. We think the change in recharge is more likely to be in the range of 600 to 850 mm.
2. Summer evapotranspiration for the forest and annual evapotranspiration for the clearcut is known relatively well compared to winter evapotranspiration for the forest, in so far as the recharge cases give fairly similar results for these fluxes.
3. Winter evapotranspiration losses are probably as large or larger than the summer evapotranspiration losses for the forest, with interception loss most likely being the dominant component.
4. Site-specific determination of leaf area index and particularly storm throughfall fraction would help to reduce the uncertainty range considerably. More information about factors affecting or probable rates of winter transpiration rates are needed.

Impacts of Harvest on Steep Slopes with Thin Soils Versus Low-gradient Slopes with Thick Soils

The following question was posed for this project: Will timber harvest from thin soils mantling steep bedrock slopes have a different impact than timber harvest from deep (glacially derived) soils on low-gradient slopes? The results of the simulation described in this paper help us to give a more informed answer. In answering this question, it is helpful to distinguish components of the water budget: summer transpiration, winter transpiration, and interception loss. The factors that determine whether site differences will occur are somewhat different for each of these three water budget components.

Both sites described are well-drained. For well-drained locations, the maximum possible evapotranspiration that can occur in summer is limited to the sum of plant available water capacity, summer season precipitation, and upward movement of moisture from below the root zone, due to capillary action. The latter quantity will usually be small, particularly for sandy soil. If shallow soil restricts rooting depth at one site, then this will limit growing season evapotranspiration at that site as compared to the other site. Assuming no difference in leaf area index and summer precipitation, summer evapotranspiration loss for the two site conditions will differ mainly on the basis of differences in plant available water capacity of the soil. This statement is valid because (1) soil moisture will almost certainly be at its maximum value every spring, regardless of site condition, and (2) because summer potential evapotranspiration is large compared to summer rainfall amount.

In winter, soil moisture can be assumed to be non-limiting to transpiration at both sites. Winter transpiration losses therefore will be sensitive to differences in leaf area index and meteorological conditions at the two sites, but not to soil moisture status. Annual interception loss is sensitive to differences in leaf area index, to potential evaporation, and to rainfall amount. Therefore, apart from differences in meteorological conditions and leaf area index that might exist, we expect that winter evapotranspiration at the two sites will not differ, and that any difference in annual evapotranspiration will arise over the summer, *i.e.* we expect annual evapotranspiration at the two sites to have a difference roughly equal to the difference in plant available water capacity.

Sensitivity analysis showed that at Hazel annual evapotranspiration for the forest was relatively insensitive to plant available water capacity over the range of 200 mm to 300 mm (RZ-max in Figure 3). This is because a 100 mm difference in capacity is small compared to the estimated magnitude of annual evapotranspiration, a large portion of which is due to interception loss. Notwithstanding any difference in annual evapotranspiration, the drainage path for water needs to be considered as well, in order to assess the effects of timber harvest for the two different site conditions.

Thinning

Wolff *et al.* (1989) pointed out that summer transpiration rates are similar for thinned stands and unthinned stands, provided that an understory is associated with the thinned stand (Black *et al.*, 1980). We did not simulate a thinned forest; however the results of the present work afford some additional insight in this issue. In particular, results of the work described herein suggest that the issue of interception loss must also be addressed when estimating the potential effect of

thinning on the annual water balance. It is likely that interception loss would be changed after thinning. Substantially lowered leaf area index should lead to an increase in the proportion of rainfall that passes through the canopy to be intercepted by understory or to reach the ground (Giles *et al.*, 1985). On the other hand, thinning may lead to better ventilation of the overstory. These effects may diminish over time as the stand recovers from thinning. To conclude that thinning has no effect on recharge or water yield is probably correct only if annual interception loss is small compared to annual transpiration, which, as we have seen, is probably not the case at Hazel. (It would be possible to simulate a thinned forest with the present model. The only parameter change would be to reduce leaf area index for the forested case to an appropriate value.)

Recommendations

The simulation results show that any effort to reduce the uncertainty range for recharge should focus on better characterization of the forest parameters. In particular,

1. Estimate winter interception losses with a regression equation (*e.g.* interception loss as a linear function of daily precipitation total), such as described by Giles *et al.* (1985). Regression equations have been found to predict most of the variability in interception loss, and their use avoids all of the difficulties and uncertainties that come with application of the Penman-Monteith equation to interception. Parameters should be determined empirically, at Hazel.
2. Estimate leaf area index on the basis of species-specific allometric equations, such as given by Gholz (1982). The only data required is a representative sample of tree diameter-at-breast height. This is a simple calculation.

Our results show that for Hazel, and likely for other lowland basins in the area, winter evapotranspiration may well be substantial and may account for a major portion of the annual water budget. This result may have important implications for the relation between landsliding potential and forest management in low-elevation basins in northwestern Washington.

Appendix I. Model description, parameter estimation

Interception loss. Interception loss was modeled by Kelliher *et al.* (1986) with the following equation:

$$\text{change in canopy store} = (1 - \text{FTHRU}) * (\text{above-canopy precip.}) - \text{Sr} * \text{PEV}$$

where FTHRU is a canopy parameter, Sr represents the amount of water on the canopy relative to capacity, and PEV is potential evaporation, calculated with the Penman-Monteith equation by setting stomatal resistance to zero. Excess storage results in drainage (Sr cannot exceed 1.0). Because of drainage, the simulated ratio of throughfall to precipitation in a given storm can exceed FTHRU.

The major difficulty in applying the interception model was found to be the estimation of the throughfall fraction FTHRU. In applying this equation to the drier climate of East Vancouver Island, Kelliher *et al.* (1986) found that an appropriate summer-season value for FTHRU to be 0.60 for a Douglas fir stand having a leaf area index of 6.0. Giles *et al.* (1985) found interception loss to be linearly related to LAI. Their data suggests that an appropriate value for FTHRU for LAI of 5.0 and 10.0 would be 0.8 and 0.4 for the East Vancouver stands. In the more humid climate at Hazel, we might expect the throughfall parameter to have a somewhat higher value at the same leaf area index.

Interception estimates for Oregon west slope Cascades is perhaps more applicable to Hazel than the East Vancouver Island data. Two different reports for rainfall-dominated forested locations in the H.J. Andrews Experimental Forest, Oregon, give large differences in interception loss within a relatively small area. Troendle and Leaf (1980) calibrated a hydrologic model to 1974 rainfall-runoff data of Watershed 2 (60 ha, elevation range 400 to 1100 m), and found that interception accounted for ‘most’ of the annual evapotranspiration loss of 47 inches at this site. Rothacher (1963) measured throughfall and gross precipitation for one year (water year 1960) in an old-growth Douglas fir plot at 1600 m (average annual precipitation 92 inches). He found that throughfall was about 80% of rainfall in winter and summer (76% in summer, 86% in winter).

The results of Troendle and Leaf (1980) imply a value for FTHRU at the H.J. Andrews site of not more than 0.50. The results of Rothacher imply a value of 0.80. For the high PET case (LAI of 10.0) we chose a value of 0.65 as a compromise between these two values. For the low PET case (LAI of 5.0), we chose a value of 0.80.

Canopy interception store capacity is calculated on the basis of leaf area index (LAI). Estimation of LAI is described below. In summer canopy interception store capacity is assumed to be $0.1 * \text{LAI}$ (Wigmosta *et al.*, 1994). We assume a somewhat lower value in winter for the evergreen cover. A small non-zero value for the deciduous cover in winter allows for the possibility of interception by exposed twigs, etc.

Aerodynamic resistance. We assume aerodynamic resistance is constant for a given vegetation cover. We recognize that for interception loss, aerodynamic resistance is a sensitive variable (McNaughton and Jarvis, 1983). A sensitivity analysis was performed to determine reasonable

maximum and minimum values for tall (20 - 40 m) and short (0.1 to 1.0 m) canopies. A range of winds speeds were considered, inclusive of the typical summer's day wind speed at the Darrington climate station (3 m/s at an instrument height of 2 m). For this analysis we assumed a logarithmic wind speed profile, stable conditions, and similarity of the roughness lengths for momentum, heat, and moisture (see Rowntree, 1991). The upper and lower parameter bounds determined in this manner are given in Table I. The parameter ranges assumed for the two covers are consistent with reported values and ranges for forest (McNaughton and Black, 1973; Gash and Stewart, 1975; Rowntree, 1991) and clearcut (Adams *et al.*, 1991; Rowntree, 1991).

Various sources indicate that for a wide variety of vegetation covers, hourly transpiration rates do not exceed about 0.40 mm/hr. We found that the simulated 6 hour transpiration rates rarely if ever exceeded this threshold.

Soil moisture accounting. As for soil moisture accounting, we take a simpler approach than Kelliher *et al.* (1986). We consider soils at Hazel to be either well-drained or poorly-drained. We assume that the clearcut would occur at a well-drained site. The unconsolidated sands that occur at Hazel would be sufficiently rapidly draining as to warrant a very simple representation of soil moisture (Linsley *et al.*, 1975). Change in storage is simply equal to throughfall less transpiration. Excess storage (additions of throughfall that would cause soil moisture in the root zone to exceed capacity) is discharged to groundwater. The stomatal resistance function ensures that the transpiration demand tends to zero as the root zone becomes desiccated. The plant available water capacity in the root zone is equated with

rooting depth*(field capacity - permanent wilting point).

Storck *et al.* (1996) evaluated digitized state and federal soils maps for the Snoqualmie River basin, WA. Assuming a rooting depth of 1.5 m for overstory, their analysis suggests values of 195 mm and 420 mm as the plant available water capacity, for glacial deposits and organic soils, respectively. We assume 250 mm as a typical value for this model parameter, with slightly higher and lower values as the upper and lower bounds. For the clearcut, we assume plant-available water capacity to be half that for the overstory, as short vegetation typically has a shallower rooting habit than tall vegetation.

Leaf area index (LAI). For the most part, LAI is the only parameter for which species differences (for similar basal area index) are likely to have a significant effect on simulated transpiration. In general, LAI varies with species, basal area index, climate, and site quality (Zobel *et al.*, 1976; Gholz, 1982; Giles *et al.*, 1985). Site quality refers mainly to factors affecting resource availability (nutrients, water, solar radiation). A typical range for all-sided LAI in a mature low elevation western Cascade Douglas fir stand (*i.e.* in the so-called Douglas fir zone), with good site quality, seems to be 17 to 24 in Oregon (Zobel *et al.*, 1976; Gholz, 1982). Values twice this were found for mixed stands at somewhat higher elevation (*i.e.* in the Western Hemlock zone), apparently due to better soil moisture availability at the end of the growing season. Assuming applicability to Hazel, and using 1:2.3 as the ratio of one-sided to all-sided LAI, the data for Oregon suggests 10 as a reasonable value for the upper bound value for this parameter. We assume 7 as a typical value, and 5 as a lower bound value.

Stomatal resistance. Tan *et al.* (1978) found that the only environmental stresses affecting stomatal resistance in summer time for a Douglas Fir stand on Eastern Vancouver Island were

vapor pressure deficit and soil moisture tension. In particular, the sensitivity to vapor pressure deficit increased as soil moisture tension increased. Furthermore, they showed that variation in stomatal resistance was not affected by thinning (and presence of a rich salal understory), and was mainly accounted for by variations in soil moisture tension and vapor pressure deficit. There is no reason to expect that similar experiments at Hazel would yield very different patterns, for Douglas fir and other naturally abundant conifer species.

Regression equations expressing the stomatal resistance behavior were provided by Tan *et al.* (1978), and these were used by Kelliher *et al.* (1986). Rather than using these equations we devised a simple function (F1) of vapor pressure deficit and plant available water (the depth of extractable water in the root zone at any particular time) that emulates the behavior of those equations. The function is applied in the form of a multiplicative model of stomatal resistance (Shuttleworth, 1991), having a parameter *rsmin* (minimum stomatal resistance for a canopy with leaf area index of one):

$$\text{canopy resistance} = \text{rsmin} / \text{F1} / \text{LAI}$$

where F1 varies between 0 and 1, and has value 1 when vapor pressure deficit and soil moisture stress are weak. The advantage of this approach is that it allows us to explore sensitivity to minimum stomatal resistance independently of soil moisture and vapor pressure deficit stress, and to calibrate the function to the study site (see Discussion). We assume the clearcut vegetation to behave similarly to salal.

Winter application. In order to apply this model to winter conditions, we make the following assumptions: (1) Among all the parameters only LAI (and canopy interception store) is seasonably variable. In winter, we assume LAI for clearcut goes to zero and that LAI for the coniferous forest decrease slightly. (2) Stomatal resistance goes to infinity when 6-hour average temperature is -2 °C (Waring *et al.*, 1978) and when 6-hour average insolation falls below 70 W/m² (Running, *et al.*, 1987).

Parameter values - clearcut

Deciduous forests and particularly short vegetation exhibits less stomatal control and less conservative water use than evergreen forests. Thus the clearcut is assigned a lower LAI (and canopy interception store) than the low PET case for forest, but is assigned somewhat lower minimum stomatal resistance, following data given by Adams *et al.* (1991) for a grass-covered forest clearcut. Because of lower leaf area index, the clearcut is assigned a higher throughfall fraction FTHRU.

Appendix II. Estimation of meteorological forcing data at Hazel

We describe briefly in this section the estimation of six-hourly forcing data. Required forcing data includes precipitation, air temperature, and dew point temperature. These variables were simulated from historic daily precipitation and daily minimum and maximum air temperatures (T_{min} , T_{max} , respectively) recorded at Darrington over the period 1931 to 1994. As discussed in the main report, the air temperature at Hazel was assumed to be the same as at Darrington. Precipitation amounts at Hazel were assumed to be 7/9 of the amount observed at Darrington. Wind speed data is not available; therefore aerodynamic resistance is treated as a model parameter (see Appendix I).

Air temperature (T_a) was estimated by assuming a sinusoidal diurnal pattern, with T_{min} occurring early morning and T_{max} occurring in early afternoon. Following Running *et al.* (1987), vapor pressure deficit is calculated, most days, as the difference in saturation vapor pressure at the 6-hourly air temperature and saturation vapor pressure at the most recently observed T_{min} (precipitation occurrence is also taken into consideration). Net radiation was estimated on the basis of latitude, Julian day, air temperature, dew point, and cloudiness, using the algorithm of Bristow and Campbell (1984). In calculating insolation, we assumed a horizontal surface, with no topographic shading, and albedos of 0.12 and 0.18 for forest and clearcut, respectively (Running *et al.*, 1987).

Storms were considered to be 18 hours in duration throughout the year and of uniform intensity during the duration of the storm. On rainy days, the period 6 p.m. to midnight was assumed to be always rain-free. We found little difference in results for a 24-hour storm duration assumption.

BIBLIOGRAPHY

- Adams, R.S., T.A. Black, and R.L. Fleming, 1991, Evapotranspiration and surface conductance in a high elevation, grass-covered clearcut, *Agricultural and Forest Meteorology*, vol. 56, p. 173-193.
- Black, T.A., C.S. Tan, and J.U. Nnyamah, 1980, Transpiration rate of Douglas-fir in thinned and unthinned stands, *Canadian Journal Soil Science*, vol. 60, p. 625-631.
- Bosch and Hewlett, 1982, A review of catchment experiments to determine the effect of vegetation changes on water yield and evapotranspiration, *Journal of Hydrology*, vol. 55, p. 3-23.
- Bristow, K.L., and G.S. Campbell, 1984, On the relationship between incoming solar radiation and daily maximum and minimum temperature, *Agricultural and Forest Meteorology*, vol. 31, p. 159-166.
- Emmingham, W.H., and R.H. Waring, 1977, An index of photosynthesis for comparing forest sites in western Oregon, *Canadian Journal of Forest Research*, vol. 7, p. 165-174.
- Fritschen, L.J., J. Hsia, and P. Doraiswamy, 1977, Evapotranspiration of a Douglas fir determined with a weighing lysimeter, *Water Resources Research*, vol. 13, no. 1, p. 145-148.
- Gash, J.H.C., and Stewart, J.B., 1977, The evaporation from Thetford Forest during 1973, *Journal of Hydrology*, vol. 35, p. 385-396.
- Gholz, H.L., 1982, Environmental limits on aboveground net primary production, leaf area, and biomass in vegetation zones of the Pacific Northwest, *Ecology*, vol. 63, p. 469-481
- Giles, D.G., T.A. Black, and D.L. Spittlehouse, 1985, Determination of growing season soil water deficits on a forested slope using water balance analysis, *Canadian Journal of Forestry*, vol. 15, p. 107-114.
- Harr, R.D., 1976, Forest practices and streamflow in Western Oregon, in *Symposium on Watershed Management*, U.S. Forest Service, PNW-GTR-49.
- Harr, R.D., R.L. Fredriksen, and J. Rothacher, 1979, *Changes in streamflow following timber harvest in Southwest Oregon*, U.S. Forest Service Research Paper PNW-249.
- Harr, R.D., A. Levno, and R. Mersereau, 1982, Streamflow changes after logging 130 year old Douglas-fir in two small watersheds, *Water Resources Research*, vol. 18, p. 637-644.
- Kelliher, F.M., T.A. Black, and D.T. Price, 1986, Estimating the effects of understory removal from a Douglas fir forest using a two-layer canopy evapotranspiration model, *Water Resources Research*, vol. 22, no. 13, p. 1891-1899.
- Linsley, R.K., M.A. Kohler, and J.L.H. Paulhus, 1975, *Hydrology for Engineers, 2nd ed.*, McGraw-Hill, New York, N.Y., 482 pp.
- McNaughton, K.G. and T.A. Black, 1973, A study of evapotranspiration from a Douglas Fir forest using the energy balance approach, *Water Resources Research*, vol. 9, no. 6, p. 1579-1590.
- McNaughton, K.G. and P.G. Jarvis, 1983, Predicting effects of vegetation changes on transpiration and evaporation, in *Water Deficits and Plant Growth, Volume VII*, T.T. Kozlowski, ed., Academic Press, p. 1-47.
- Monteith, J.L., 1965, Evaporation and environment, *Symp. Soc. Exp. Biol.*, vol. 19, p. 205-234.
- Pearce, A.J., J.H.C Gash, and J.B. Stewart, 1980a, Rainfall interception in a forest stand estimated from grassland meteorological data, *Journal of Hydrology*, (Amsterdam) vol. 46, p. 147-163.
- Pearce, A.J., L.K. Rowe, and F.B. Stewart, 1980b, Nighttime, wet canopy evaporation rates and the water balance of an evergreen mixed forest, *Water Resources Research*, vol. 16, no. 5, p. 955-959.
- Reed, K.L. and R.H. Waring, 1974, Coupling of environment to plant response: a simulation model of transpiration, *Ecology*, 55, p. 62-72.

- Rothacher, J., 1963, Net precipitation under a Douglas-fir forest, *Forest Science*, vol. 9, no. 4, p. 424-429.
- Rothacher, J., 1970, Increases in water yield following clearcut logging in the Pacific Northwest, *Water Resources Research*, vol. 6, p. 653-658.
- Rowntree, P.R., 1991, Atmospheric parameterization schemes for evaporation over land: Basic concepts and climate modeling aspects, in *Land Surface Evaporation, Measurement and Parameterization*, T.J. Schmugge and J.C. Andre, eds., Springer-Verlag.
- Running, S.W., R.R. Nemani, R.C. Hungerford, 1987, Extrapolation of synoptic meteorological data in mountainous terrain, and its use for simulating forest evapotranspiration and photosynthesis, *Canadian Journal of Forest Research*, vol. 17, p. 472-483.
- Rutter, A.J., K.A. Kershaw, P.C. Robins, and A.J. Morton, 1971, A predictive model of rainfall interception in forests, 1. Derivation of the model from observations in a plantation of Corsican Pine, *Agricultural Meteorology*, vol. 9, p. 367-384.
- Rutter, A.J. and A.J. Morton, 1977, A predictive model of rainfall interception in forests, III, Sensitivity of the model to stand parameters and meteorological variables, *Journal of Applied Ecology*, vol. 14, p. 567-588.
- Shuttleworth, W.J., 1991, Evaporation models in hydrology, in *Land Surface Evaporation, Measurement and Parameterization*, T.J. Schmugge and J.C. Andre, eds., Springer-Verlag.
- Stednick, J.D., 1996, Monitoring the effects of timber harvest on annual water yield, *Journal of Hydrology*, vol. 179, p. 79-95.
- Storck, P., D.P. Lettenmaier, B.A. Connelly, and T.W. Cundy, *Implications of forest practices on downstream flooding, Phase II Final Report*, Washington Forest Protection Association, 1996.
- Tan, C.S., T.A. Black, and J.U. Nnyamah, 1978, A simple diffusion model of transpiration applied to a thinned Douglas-fir stand, *Ecology*, vol. 59, no. 6, p. 1221-1229.
- Troendle, C.A., and C.F. Leaf, 1989, Chapter III: Hydrology, in *An Approach to Water Resources Evaluation of Non-Point Silvicultural Sources*, U.S. Environmental Protection Agency, EPA-600/8-80-012.
- Waring, R.H., W.H. Emmingham, H.L. Gholz, and C.C. Grier, 1978, Variation in maximum leaf area of coniferous forests in Oregon and its ecological significance, *Forest Science*, vol. 24, no. 2, p. 131-139.
- Whitehead, D. and F.M. Kelliher, 1991, A canopy water balance model for a *Pinus radiata* stand before and after thinning, *Agricultural and Forest Meteorology*, vol. 55, p. 109-126.
- Wigmosta, M.S., L.W. Vail, and D.P. Lettenmaier, 1994, A distributed hydrology-vegetation model for complex terrain, *Water Resources Research*, vol. 30, no. 6, p. 1665-1679.
- Wolff, N., M. Nystrom, S. Bernath, 1989, *The Effects of Partial Forest-stand Removal on the Availability of Water for Groundwater Recharge*, report prepared for State of Washington, Department of Natural Resources.
- Zobel, D.B., A. McKee, G.M. Hawk, C.T. Dyrness, 1976, Relationships of environment to composition structure, and diversity of forest communities of the central western Cascades of Oregon, *Ecological Monographs*, vol. 46, p. 135-156.

Stability Assessment of the Hazel Landslide

Dan Miller

This analysis uses quantitative models of the physical processes acting on the Hazel landslide to better elucidate the factors controlling landslide behavior. These models use existing or easily obtained site-specific information. We have adapted existing models and developed new ones for this purpose. A geographical information system (GIS) is used to store and organize the information, to provide data to the numerical models, and to display model results.

The behavior of the landslide, the characteristics of the material in which it occurs, and the nature of the mass wasting processes have been described in Section 1 of this report and in previous reports and memoranda (Shannon and Associates, 1952; Thorsen, 1969; Wolff, 1988; Benda et al., 1988; DNR, in prep). These investigations identified two factors controlling behavior of the landslide over time:

- 1) Erosion of material from the toe by the Stillaguamish River, and
- 2) Variations in groundwater flux to the landslide.

Land use in the vicinity of the landslide has been discussed as a factor potentially affecting landslide behavior because of the reduction in evapotranspiration and consequent potential increase in groundwater recharge associated with timber harvest (e.g., Wolff, 1988; Benda et al., 1988). Hence, three types of models are used to characterize processes controlling landslide behavior: an evapotranspiration model, a groundwater model, and a model of deep-seated mass wasting. Given the range of complexity to be found in such models currently available, those used are relatively simple. Simple models are chosen for two reasons: computational efficiency and minimal data requirements. The groundwater and mass-wasting models are described separately below; the evapotranspiration model was described in Section 2.

The Groundwater Model

A finite-element groundwater model written by and available from the U.S. Geological Survey was used for this work. This model, MODFE, was chosen because the source code is freely available (Torak, 1993a; also over the internet at <http://h2o.usgs.gov/software>), it is well documented (Cooley, 1992; Torak, 1993b), and it has a history of use (Buxton and Modica, 1992; Czarnecki and Waddell, 1984; Iverson and Reid, 1992; Reid and Iverson, 1992; Torak et al., 1992). MODFE is a two-dimensional finite-element model using linear, triangular elements. It can simulate both steady-state and transient groundwater flow in unconfined aquifers and can accommodate seepage at the ground surface. However, certain modifications were required for this problem. The program was modified to simulate flow through a multilayered unconfined aquifer (here the coarse, permeable outwash deposits overlying fine, low-permeability lacustrine silts) and to recognize a seepage face. Data for each node of the finite-element mesh were taken from GIS data files. The GIS used is IDRISI: an inexpensive, PC-based set of programs available from Clark University. Pre- and post-processors (computer programs) were written to transfer data between the GIS and the groundwater model.

Data Requirements: Site Characterization

As described in Section 1, groundwater flow to the Hazel landslide occurs primarily within an aquifer formed by the glacial outwash deposits composing the terrace remnant known as the Whitman Bench (Figure 1.2). Seepage observed emanating from slopes adjacent to Rollins Creek and from slopes defining the south-east edge of the Whitman Bench indicate that groundwater flow to the landslide originates from recharge confined to an area bounded to the east and north by Rollins Creek and to the south by the Stillaguamish River. The potential westward extent of the regional flow field affecting groundwater movement toward the Hazel landslide is unknown. As discussed in Section 1, we infer that the westward watertable divide occurs somewhere within the Whitman Bench. To insure that the divide is included within the boundary of the finite-element mesh, the westward boundary of the mesh was placed well away from the area of interest, as shown in Figures 1.1 and



1.2. Subsequent model runs indicate that the mesh boundary is sufficiently far from the calculated recharge area to the landslide to have no effect on model results.

A simplified representation of the aquifer is used in the model to simulate groundwater flow. The aquifer is viewed as an isotropic, homogeneous deposit of sand of varying thickness, underlain by an isotropic, homogeneous, fine-grained deposit of clay. The contact between these two deposits is considered continuous and distinct and occurs at an elevation that may vary from point to point. The aquifer is characterized in terms of transmissivity, a measure of the potential horizontal flux of groundwater below a point on the ground surface, and specific yield, a measure of the change in volume of water stored within the aquifer caused by a unit change in watertable elevation. Transmissivity is calculated by multiplying the saturated thickness of the sand layer, determined as the difference between the water table and sand/clay contact elevations, by the saturated hydraulic conductivity of the sand. Groundwater flow is allowed within the clay layer, although at a much smaller rate. The data required to characterize the aquifer are elevations of the ground surface, elevations of the sand/clay contact, and the saturated hydraulic conductivity and specific yield of the sand and clay.

Elevations are represented by a uniform, square grid of points in the GIS. The primary source for surface elevations is a 1:4800-scale topographic map made from 1978 aerial photography. Contour lines from a portion of this map were digitized and provided by DNR. Elevations for areas not included were obtained from 30-meter digital elevation models (DEM) for the Oso and Mount Higgins 7½-minute quadrangles available from the USGS. Data from these two sources were merged and splined to a uniform 10-meter grid. Each square grid cell comprised two triangular elements of the finite-element mesh.

Elevations of the sand/clay contact are somewhat harder to determine than those of the ground surface. The depositional setting (a proglacial lake followed by a broad outwash plain) suggests that the original surface was relatively flat. Subsequent fluvial and glacial processes have disrupted this surface and left multiple channel and shallow lake deposits within the stratigraphy so that a single, well-defined contact is not found at all points. The resulting vertical heterogeneity is not really a problem, since the model works in terms of horizontal transmissivity. Localized deposits of low permeability result in perched groundwater that are not accounted for in the model, but these zones probably have little influence on regional patterns of groundwater flow. (Nevertheless, perched groundwater may be locally important to slope stability.) Additionally, the original contact surface may have been tilted by regional tectonic uplift. Indeed, the surface of the Whitman Bench tilts slightly to the north (DNR, in prep). Having few measurements of actual contact elevations, however, we approximate the undisturbed contact as horizontal.

The original stratigraphy has been subsequently disrupted by mass wasting. The margins of the Whitman Bench have a scalloped morphology indicative of large-scale slumping. As discussed in Section 1, the Hazel landslide occurs on one of these large slump blocks and topography indicative of adjacent slumps occurs to the north (Headache Creek basin) and to the west (Figure 1.2). These slumps apparently carried the former stratigraphy at least partially intact as they moved, since outwash deposits still largely cover the surface of the slump blocks (as illustrated with the sketch in Figure 1.3). The elevation of the sand/clay contact varies between slump blocks. These elevations were estimated from locations of surface exposures of the contact mapped during site visits and from the four borehole logs reported in the Shannon report (Shannon and Associates, 1952). Movement of these slumps most likely involved some rotation, but lacking further subsurface information, the contact is assumed to be horizontal within a slump block. Based on surface topography and field mapping, four separate slump blocks were delineated. The inferred contact elevations used in the groundwater model are shown in Figure 3.1.

Values for saturated hydraulic conductivity and specific yield complete characterization of the aquifer. These values are constrained within the range of values reported for similar materials (e.g., Koloski et al., 1989) and were adjusted until the model simulation produced a spatial pattern of surface saturation and seepage similar to that observed in the field. The values used are reported in Table 1.



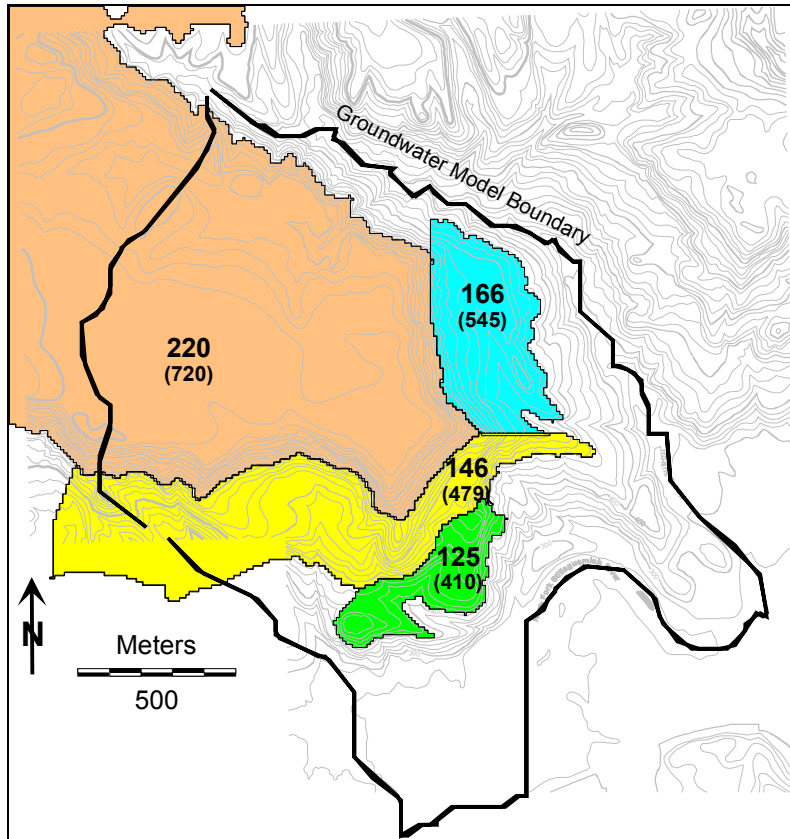


Figure 3.1. Elevations in meters (feet) assigned to the sand/clay contact. The 220-meter surface is in-place; lower elevations occur on down-dropped slump blocks (Figure 1.2). Clay is exposed at the surface in uncolored areas within the groundwater model boundary.

Simulated Recharge

The variable driving groundwater flow is recharge. The evapotranspiration model produces a 60-year time series (the duration of the precipitation record) of daily recharge estimated for the Hazel site for a given vegetation cover. For the analyses presented here, recharge was held uniform over the entire surface area of the groundwater model with changes occurring only in time. The mean annual recharge value is used for a steady-state analysis. The calculated water table elevations represent the flow field that occur in the model for a recharge that is constant year round. The steady-state solution is then used as the starting point for transient analyses, which use the simulated time series of daily recharge.

Steady-state recharge simulations were performed for both forested and clearcut conditions. As explained in Section 1, a variety of simulations were performed to determine the range of uncertainty in recharge associated with the potential range of model parameter values.

We ran groundwater simulations using the full range of potential recharge values to examine both the least- and most-stable cases.

Calculated Quantities

The model calculates the elevation of the water table for all nodes of the finite-element mesh. These values are fed back to the GIS to generate a watertable surface. A steady-state analysis produces a single surface corresponding to continuous recharge constant over time; a transient analysis produces a water table surface for each time step and illustrates aquifer response to a time series of recharge events. (MODFE was modified for this analysis to automatically adjust time steps to maintain numerical stability: time steps ranged from an imposed maximum of 2.4 hours to less than a minute, depending on the rate of change of daily recharge.) The watertable surface is used to calculate the pore-pressure distribution used by the stability model described below and to determine groundwater flow directions, from which the recharge area to specific points can

Table 1. Material Properties	Outwash Sands	Lacustrine Clays
Saturated Conductivity	0.36 m/hr	0.00036 m/hr
Specific Yield	0.25	0.1
Bulk Density (dry)	1870 kg/m ³	2020 kg/m ³
Bulk Density (saturated)	2120 kg/m ³	2120 kg/m ³
Angle of Internal Friction	38°	23°
Cohesion	5 kPa	14 kPa

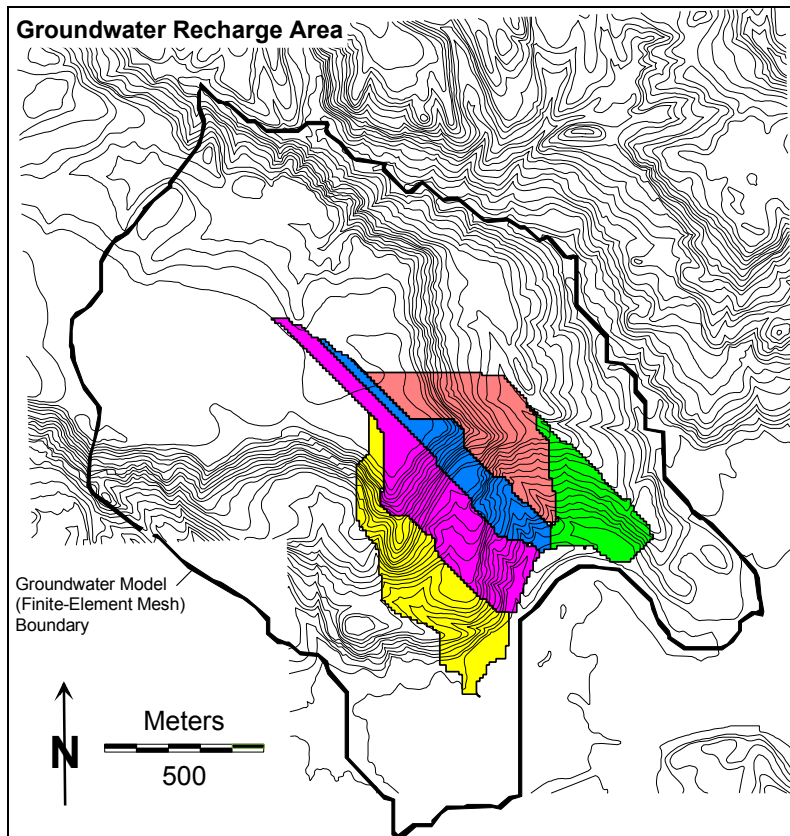


Figure 3.2 Calculated groundwater recharge area to the Hazel landslide. Different colored polygons delineate distinct zones of groundwater flow, with recharge occurring in upslope areas and discharge in downslope areas. Together these polygons bound the entire recharge area to the slide.

although not extending as far into Whitman Bench). The recharge area estimated here is obtained with an objective and repeatable model, but is based on limited field data. A true test of this prediction requires measurements of watertable elevations.

The size of the calculated recharge area varied little with changes in recharge. This result was obtained, however, under conditions of spatially uniform recharge. The recharge area may expand and contract in response to spatial variations in recharge. For example, clearcutting of Whitman Bench to the west would cause a localized increase in underlying watertable elevations, potentially causing the recharge area to the Hazel slide to expand westward. Likewise, clearcutting of Headache Creek basin may cause northward expansion of the orange-colored zone in Figure 3.2. Such scenarios were not examined in this project, but could be addressed with the tools available.

The groundwater model also allows us to separate recharge areas to different parts of the landslide, as shown by the different polygons in Figure 3.2. This ability proves useful for evaluating observed correlations between upslope harvest and landslide activity.

be delineated, as shown for the Hazel landslide in Figure 3.2 (using the steady-state, fully forested simulation). Hence, this type of model offers an estimate of the recharge area to a landslide, the second of the three questions posed by the Level 1 analysis team. Although not used in this analysis, groundwater flux can also be calculated, from which the volumetric flow of surface seepage can be estimated.

The Groundwater Recharge Area

As discussed by Freeze and Cherry (1979), the watertable forms a subdued replica of surface topography. As shown in Figure 3.2, in areas of low topographic relief and variable subsurface stratigraphy, groundwater drainage divides do not necessarily correspond to surface drainage divides. The recharge area to the Hazel slide extends farther northwest into Whitman Bench and north into Headache Creek basin than the surface divides would indicate. (Nevertheless, Benda et al., 1988, estimated a groundwater recharge area quite similar to that found in this analysis,

The Stability Model

Slope stability is characterized in terms of the potential for downslope movement of material. Gravity acts to move material downslope; movement is resisted by the material shear strength. The ratio of forces acting to move material to those acting to hold it in place define a factor of safety. Larger factors of safety indicate more stable slopes. We calculate factors of safety along linear slope transects using Bishop's simplified method of slices (Bishop, 1955), in which movement is assumed to occur along a well-defined slip surface. Data for a given transect are obtained from GIS grid files specifying elevation of the ground surface, the sand/clay contact, and the calculated water table, as shown in Figure 3.3. Material properties for the outwash and underlying clay are constrained within the range of values reported for these and similar materials (Shannon and Associates, 1952; Palladino and Peck, 1972; Koloski et al., 1989) and were back calculated for several slopes on the landslide. Values used are reported in Table 1. The minimum factor of safety is calculated for each point along the transect, as illustrated in Figure 3.3. This procedure is repeated for many transects (2000 for the examples here), so that each cell is traversed by multiple transects. Each cell is assigned the factor of safety of the least stable transect that intersects it. These methods are more fully elaborated in Miller (1995). The resulting spatial pattern of slope stability is a function of surface topography, subsurface stratigraphy, the pore-pressure distribution, and material bulk density and shear strength.

Spatial Patterns of Slope Stability

Figure 3.4 shows the factors of safety calculated for the Hazel landslide for steady-state mean-annual recharge under forested conditions. Here we use the factor of safety as a measure of relative stability: lower values indicate less stable slopes. We predict large variation in stability over the area of the landslide; a prediction that will be tested against observations of landslide behavior subsequent to the 1978 photography (on which the topography is based). The results displayed represent the influence of the topography, the calculated pore pressures, and the inferred subsurface geometry represented in the model.

These are not the only factors affecting landslide behavior, however. Spatial variation of the geotechnical properties of the clay and sand, temporal variation of pore pressures, and changes of topography that occur as portions of the landslide move may all be of equal importance in determining slope stability. These last two, temporal changes in pore pressures and topography, are examined to a limited extent below. The first, however,

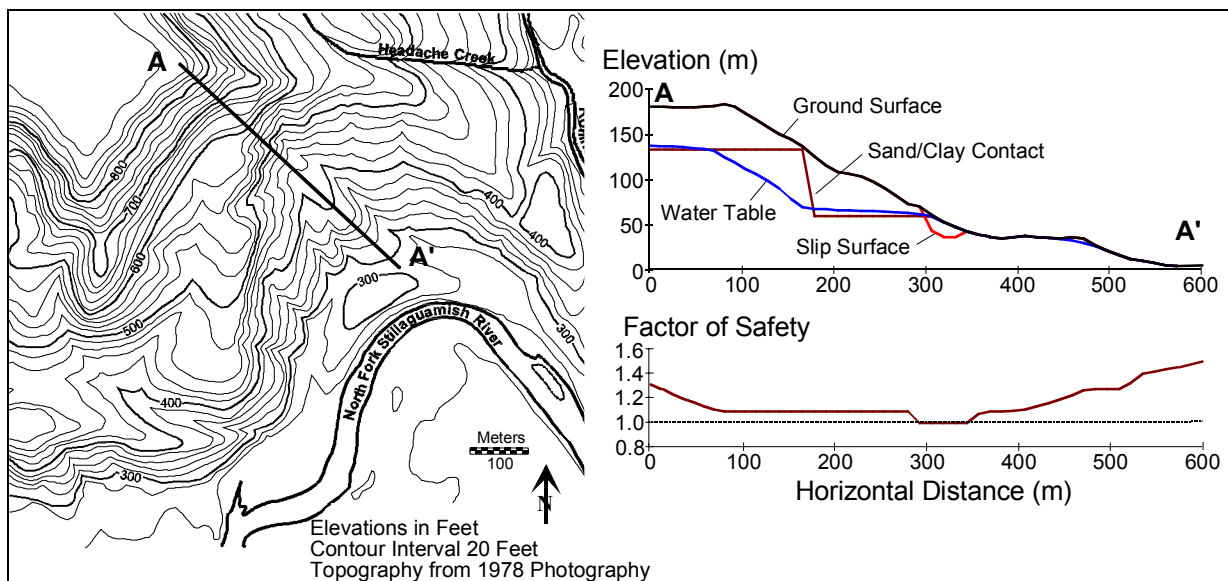


Figure 3.3. Slope transects. Cross sections for any transect are interpolated from GIS grid files. Cross-sectional data are used to calculate a profile of the minimum factor of safety along the transect. Thousands of transects are examined to produce a stability map.

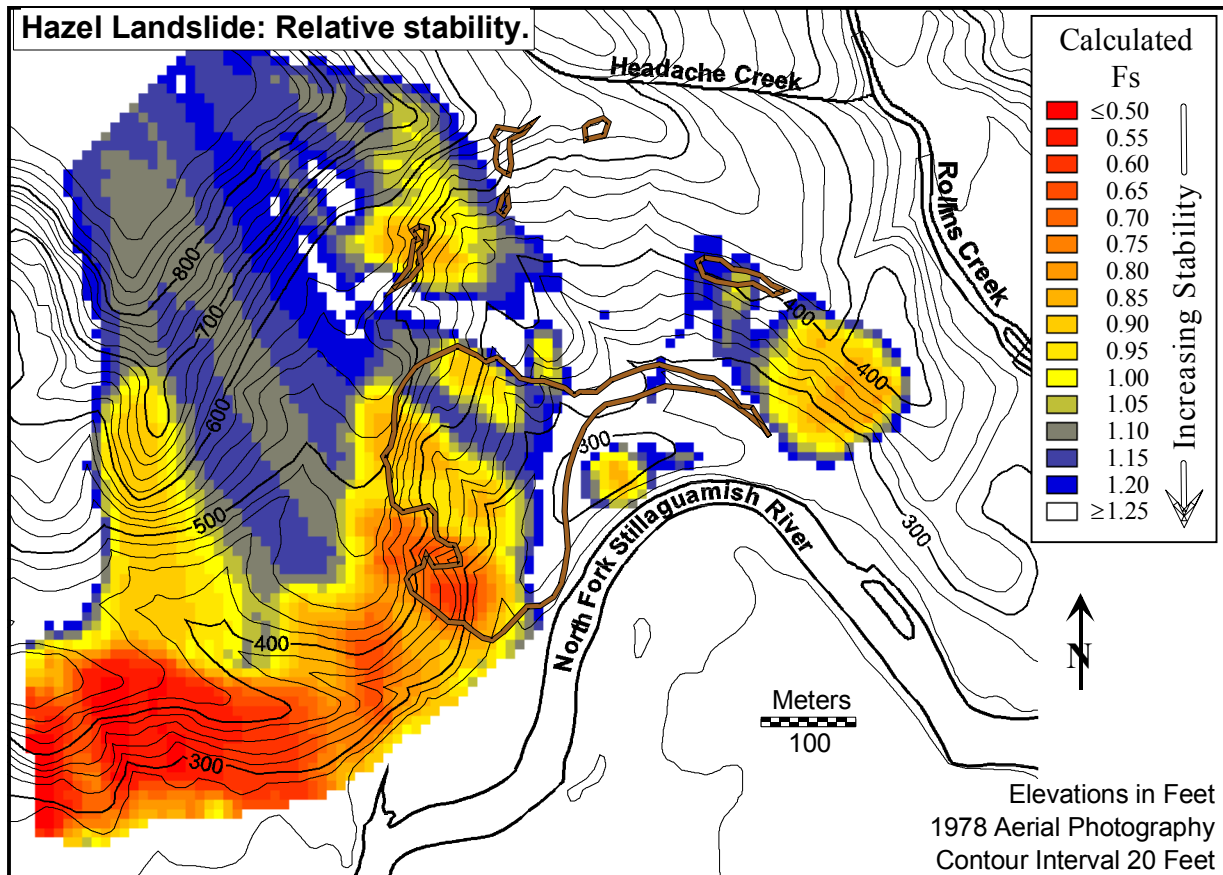


Figure 3.4. Factor-of-safety map calculated for the Hazel landslide. We use such calculations, not as a measure of absolute stability, but as a means of inferring relative stability. Indeed, as discussed in the text, factor of safety values are overestimated in disturbed areas and under estimated in undisturbed areas. Hence the low factors of safety predicted for apparently stable slopes to the west of the landslide. Note also that comparison of these results should be made only to post 1978 activity, since the topography used in the model is based on 1978 aerial photography. Heavy brown lines indicate approximate locations of landslide activity seen in the 1991 photographs (Figure 1.4).

presents a dilemma. In addition to the intrinsic heterogeneity of the outwash and lacustrine deposits, there is also a large difference between the strength of intact and disturbed material. Examining a similar deposit, Palladino and Peck (1972) report a peak strength represented by a cohesion of 0.65 ton/ft^2 and a friction angle of 35° for intact clay, compared to a residual strength represented by a cohesion of zero and a friction angle of from 13.5° to 17.5° for disturbed clay. Similar reductions are expected for the lacustrine clays at Hazel, yet we apply a single set of parameter values uniformly, using the same value for both intact and disturbed material. We have no other practical choice: even meticulous field mapping cannot resolve the three-dimensional boundaries between disturbed and in-place material. Hence, we invariably overestimate stability for disturbed deposits and underestimate stability for undisturbed deposits. The values used, obtained by back-calculations on both failed and unfailed slopes, are a compromise, and fall between the peak and residual values reported by Palladino and Peck (1972).

Unresolved spatial heterogeneity is a confounding factor that may render predicted factor-of-safety values less reliable than desired. Fortunately, we can skirt this problem to some extent by examining the predicted change in the factor of safety that occurs in response to environmental perturbations, rather than the actual factor-of-safety values themselves. The proportional decrease in stability caused by an increase in recharge, for example, or cutting of the slope toe, primarily reflects the effect of the change, with less dependence on the geotechnical

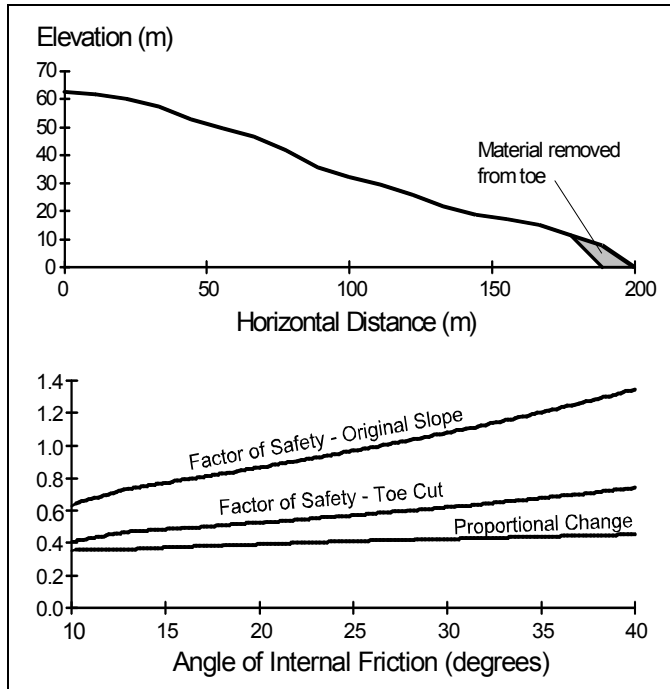


Figure 3.5. Slope sensitivity. The calculated factor of safety is strongly dependent on the geotechnical properties assigned to the slope. The magnitude of the response to a change in topography or pore pressures is much less sensitive to the assigned geotechnical properties, however, and serves as a robust gage of landslide sensitivity.

pacts of increasing recharge associated with timber harvest to those of river erosion of the toe, a primary goal of this work.

Sensitivity to Changes in Recharge

A portion of water falling as precipitation is returned to the atmosphere by evapotranspiration; a portion flows overland to stream channels, either exfiltrating as shallow subsurface return flow or falling directly on saturated or impermeable areas; and the remainder infiltrates to recharge groundwater in underlying aquifers. The depth of precipitation varies greatly from year to year; recharge to groundwater likewise varies. Vegetation, trees in particular, greatly influence processes of evapotranspiration. The effect of logging on the partitioning of water between these three flow paths is overprinted on seasonal and annual variability. We address temporal variability later; here we evaluate the magnitude and spatial distribution of landslide response to vegetation-related changes in groundwater recharge.

We use steady-state analyses, one at the simulated mean recharge rate for forested conditions and one for clearcut conditions. We calculate factors of safety for each case and then evaluate the change in stability with Equation (1). Because of uncertainty in the change in recharge between forested and clearcut conditions, this exercise is performed for two cases: 1) for that giving the least change in recharge (the highest estimated recharge under forested conditions verses the smallest estimated recharge under clearcut conditions), and 2) the greatest change (the lowest estimated recharge under forested conditions verses the greatest estimated recharge under clearcut conditions). Results are shown in Figures 3.6a and b.

property values assigned to the material. This is illustrated in Figure 3.5, which shows the minimum factor of safety calculated for a slope entirely in the clay. The change in the calculated factor of safety caused by cutting of the slope toe varies over a large range depending on the angle of internal friction assigned to the clay. The *proportional* change, however, changes little with changing friction angle. Hence we use the proportional change, calculated as

$$\frac{(F_{S_1} - F_{S_2})}{F_{S_1}} \quad (1)$$

(where F_{S_1} and F_{S_2} are the factors of safety prior and subsequent to a perturbation, respectively), as an indicator of landslide response that is less sensitive to errors in the assigned geotechnical properties than the factor of safety values themselves.

The change of stability in response to an environmental perturbation serves also as a gage of landslide sensitivity: we can evaluate the magnitude and spatial distribution of effects resulting from a change in any model variable. Hence, calculations of sensitivity, using Equation (1), allow us to compare the potential im-

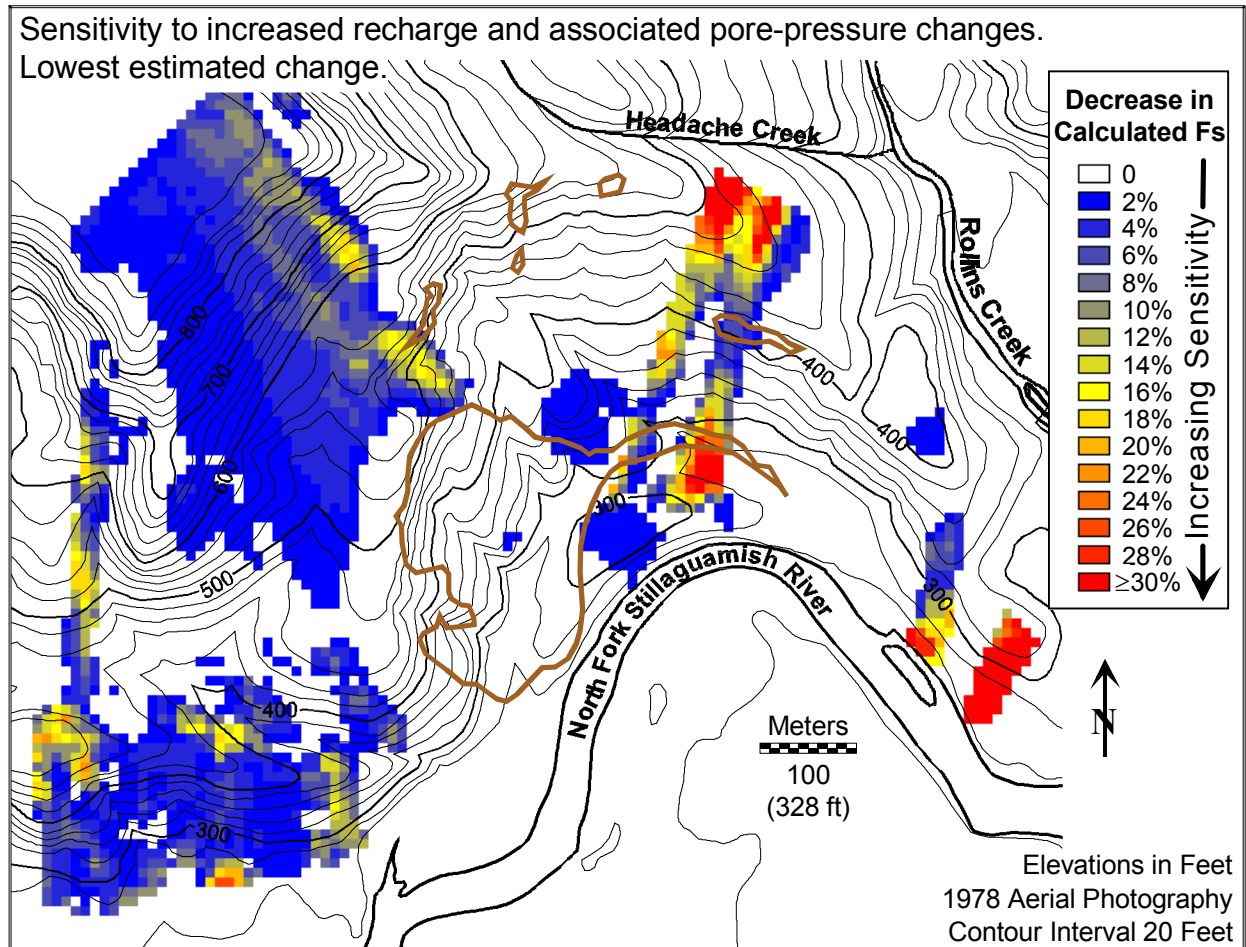


Figure 3.6a. Sensitivity to changes in recharge caused by clearcutting, *minimum* estimated change. Grid cells predicted to be stable, defined as a factor of safety of 1.3 or greater in the least stable case, are left uncolored. Heavy brown lines indicate approximate locations of landslide activity seen in the 1991 photographs (Figure 1.4).

High sensitivity to increases in recharge does not necessarily indicate that the landslide will be affected: a very stable, but sensitive slope, will be stable in either case. Thus grid cells predicted to be stable, as defined by a factor of safety of 1.3 or greater in the least stable case (F_{s2} in Equation 1), are excluded from these maps.

The resulting maps of sensitivity indicate that certain portions of the landslide will probably respond to changes in recharge differently than others: many areas are unaffected, while others experience a substantial decrease in stability. The pattern revealed is a consequence of 1) the convergence and divergence of groundwater flow, which causes spatial variability in the pore-pressure change between forested and clearcut conditions in the recharge area, and 2) variability of the surface and subsurface geometry, which causes a unique response from each slope to a change in pore pressures.

For this analysis we used spatially uniform recharge values, yet the spatial distribution of vegetation type (e.g., species, stand age) and soil parameters will produce spatial variations in evapotranspiration and corresponding recharge rates. One can, however, use these results to estimate spatial correlations between areas of recharge and landslide response. Compare the pattern of sensitivity shown in Figures 3.6 to the recharge zones delineated for different portions of the landslide in Figure 3.2. Different parts of the landslide respond to separate recharge zones, hence a change in vegetation through a portion of the recharge area, a harvest unit, for example, will likely affect only a certain portion of the landslide.

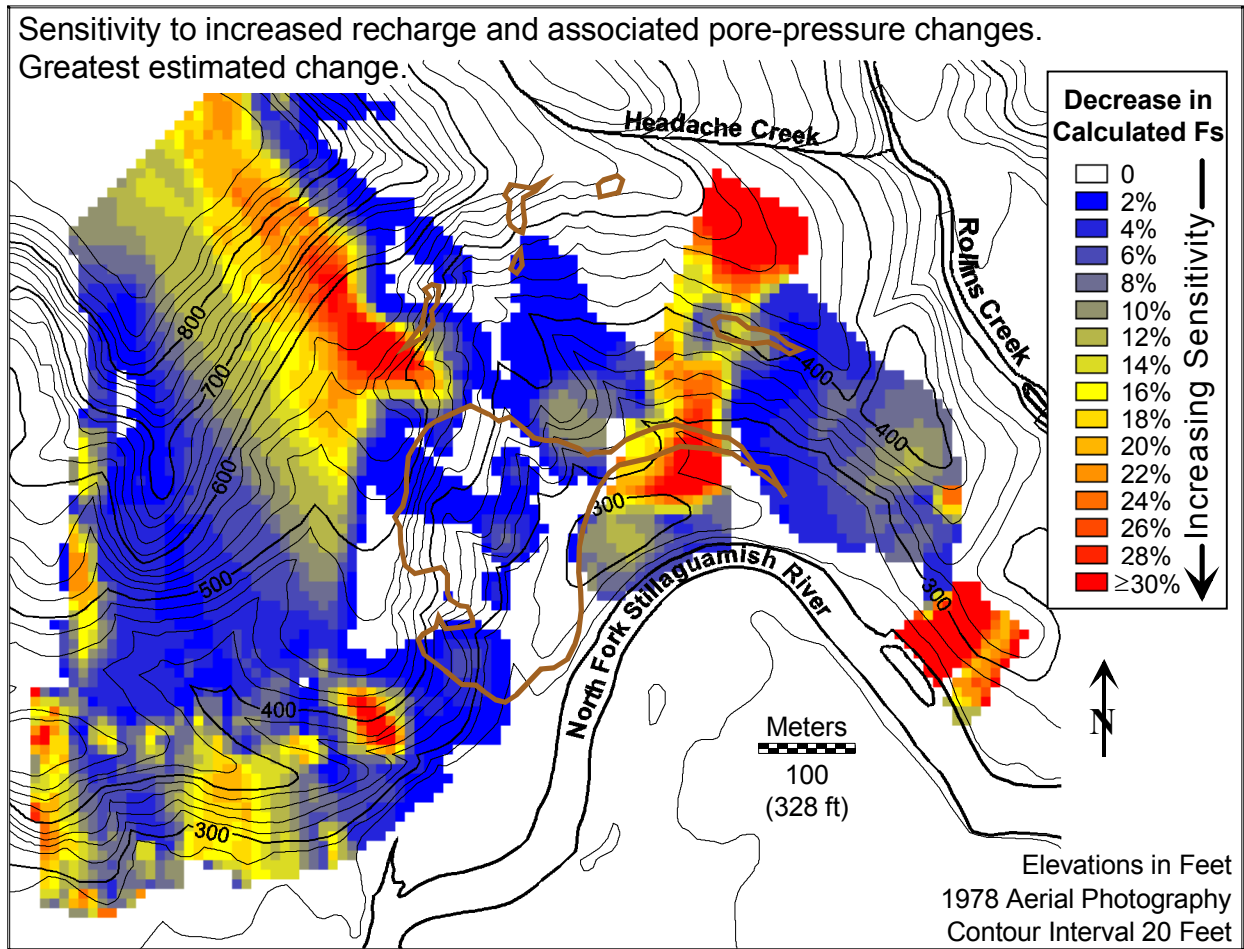


Figure 3.6b. Sensitivity to changes in recharge caused by clearcutting, *greatest* estimated change. Grid cells predicted to be stable, defined as a factor of safety of 1.3 or greater in the least stable case, are left uncolored. Heavy brown lines indicate approximate locations of landslide activity seen in the 1991 photographs (Figure 1.4).

Sensitivity to Cutting of the Slope Toe

Large, active landslides eating into the remaining glacial deposits, such as that at Hazel, invariably occur along the outside of bends where the river impinges on the margin of the terrace (DNR, in prep). This observation indicates that the river dictates where such landslides occur. Erosion of the terrace toe creates relief and slope gradients conducive to mass wasting and serves both to initiate and prolong landslide activity. Yet, once these conditions are created, the landslide likely responds both to further erosion at the toe and to pore-pressure changes caused by changing patterns of recharge. Our goal here is to delineate these responses: to separate effects of toe cutting from those of variable recharge and compare the relative influence of each. If the landslide responds primarily to what happens at the toe, with pore-pressure changes being of secondary importance, then changes in recharge have less impact than changes in the erosive potential of the river. Separating these effects allows land management and mitigation efforts to focus on the factors of greatest consequence.

To evaluate the effects of bank erosion at the toe, we simply “removed” material from the model and moved the river edge to its approximate 1984 location. We then recalculated the factors of safety for this modified topography and used Equation (1) as a measure of the change. Results are shown in Figure 3.7. Again, the response is

spatially variable. The pattern seen is a function of surface and subsurface geometry: different slopes respond differently.

Spatial variability in the responses to increased recharge and to bank erosion at the toe hinders direct comparison of the two factors. Each tends to affect different portions of the landslide. Yet the scale in Figure 3.7, showing a maximum change on the order of 75%, indicates the potential for a greater reduction in stability associated with toe cutting than found for increased recharge, for which the maximum reduction was in the range of 30%. Bank erosion produced such large changes only at the slope toes, however; upslope response is actually greater in response to increased recharge.

Of some importance is the result that cutting of the toe might destabilize slopes throughout a large portion of their length, particularly over the eastern portion of the landslide. We find a reduction in stability predicted for potential slump blocks extending all the way to Headache Creek. Headward advance and capture of Headache Creek were concerns voiced in both the Shannon report of 1952 and the Benda et al. report of 1988. Although the active scarp has advanced little since the 1967 event, tension cracks and steps indicative of Hazel-ward slumping are found along the ridge crest separating Hazel from the Headache Creek basin. Such areas of incipient slumping observed in the field are shown in Figure 3.7. The southeast-most area is also contained in an area of sensitivity to recharge indicated in Figures 3.6; the northern-most area is not. Interpretation of these features

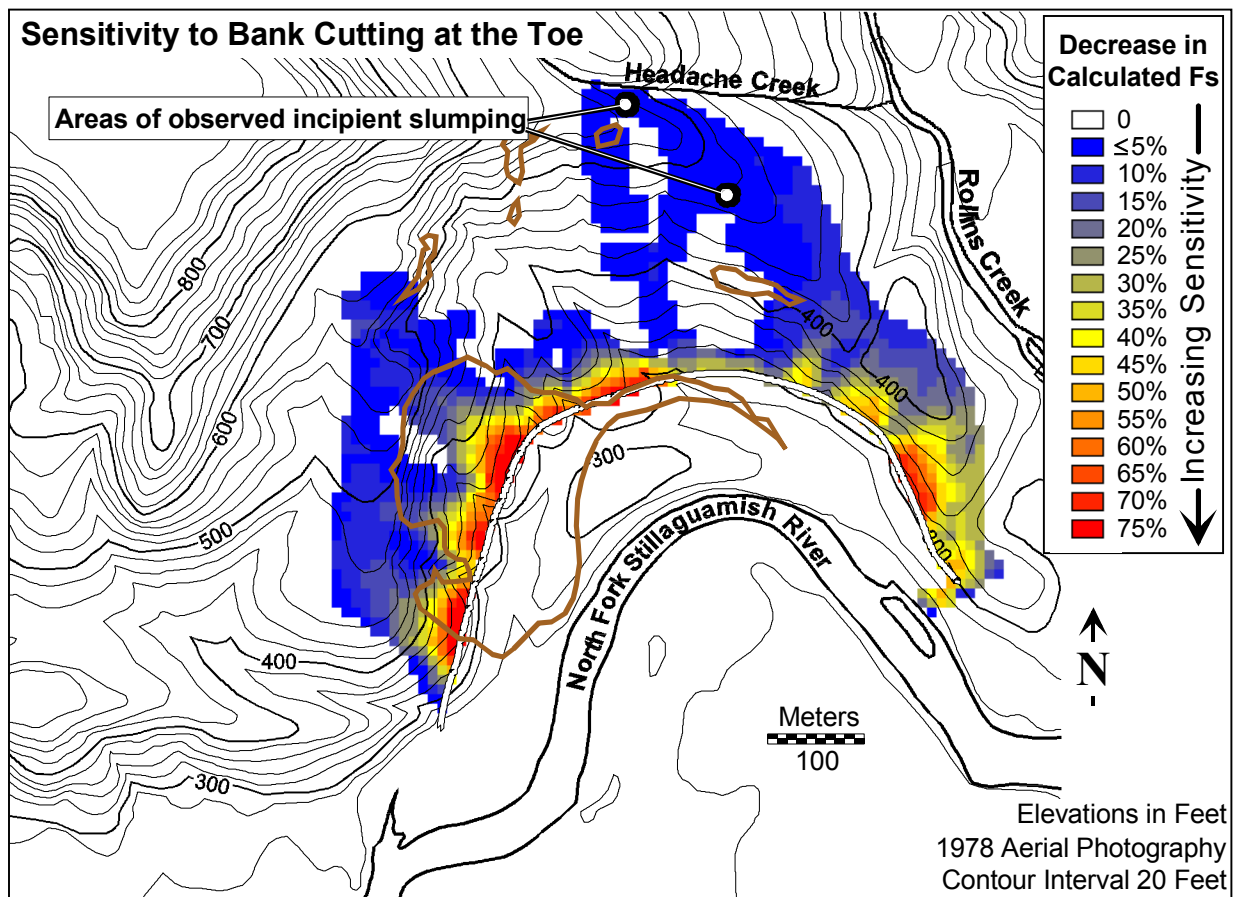


Figure 3.7. Sensitivity to cutting of the landslide toe by the Stillaguamish River. The heavy line shows the limit of bank cutting imposed for the calculation. Again, grid cells having a factor of safety of 1.3 or greater in the least stable case are left uncolored. Heavy brown lines indicate approximate locations of landslide activity seen in the 1991 photographs (Figure 1.4).

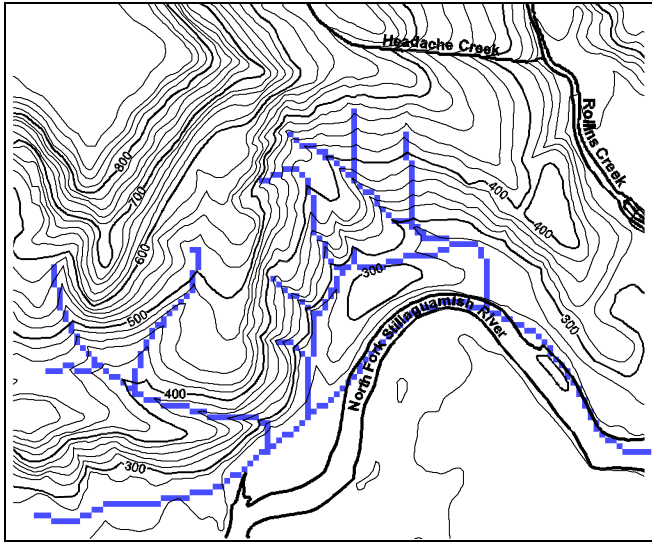


Figure 3.8. Channels draining the body of the landslide as delineated from the DEM.

is not entirely straightforward, however, because field observations indicate another potential cause of piecemeal slumping within the landslide, incision of channels draining the body of the landslide.

Sensitivity to Channels Incised Over the Body of the Landslide

Several small streams drain the body of the landslide. Their channels are lined, in places, by adjacent slumps and persistent mud flows. Evidence of channel incision (noted also by Shannon and Associates, 1952) and bank cutting suggests that these mass-wasting features are initiated and frequently reactivated by fluvial erosion of the channels. Small-scale slumping into these channels appears to occur throughout the winter months, with fluvial flushing of the fine-grained debris into the Stillaguamish year round. Over time these minor topographic readjustments and the continual removal of

material may act to destabilize larger portions of the landslide, thus activating larger slumps. We evaluate the effects of this process on landslide stability below.

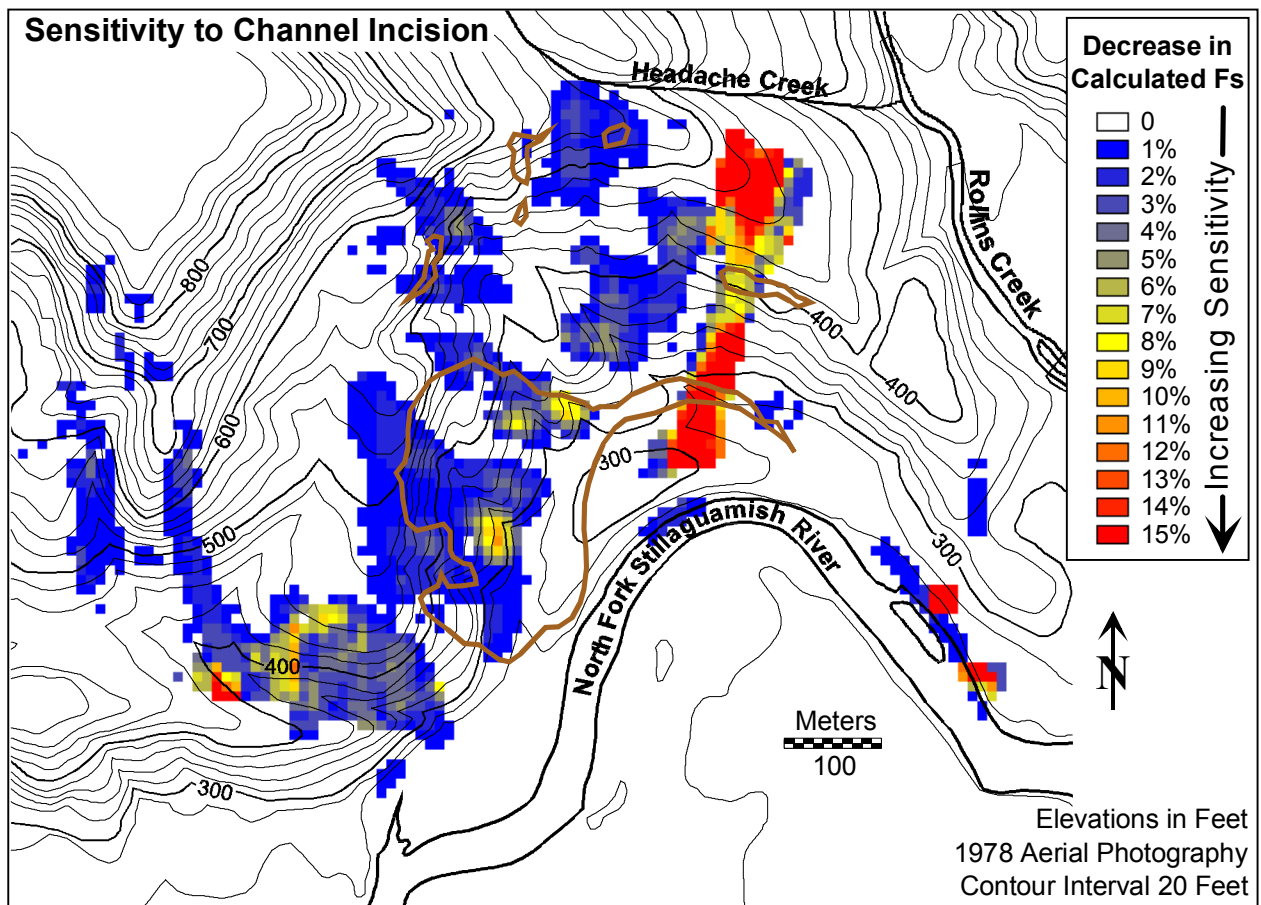


Figure 3.9. Sensitivity to incision of channels draining the body of the landslide. Grid cells having a factor of safety of 1.3 or greater in the least stable case are left uncolored. Heavy brown lines indicate approximate locations of landslide activity in 1991.

We use the 10-meter DEM to delineate channels on the landslide as shown in Figure 3.8. Channel-head locations are estimated from their current locations. We then digitally incise every channel one meter and recalculate factors of safety over the landslide. (Watertables would be unaffected by this incision, since these areas of the landslide are areas of groundwater discharge and are saturated to the surface year round). The effects of this incision are displayed, via Equation (1), in Figure 3.9. The reduction in stability is spatially variable and of the same magnitude as that found both for increasing recharge and, in upslope areas, for bank cutting by the Stillaguamish. Notably, both areas of incipient slumping shown in Figure 3.8 are included in zones affected by channel incision indicated in Figure 3.9.

Discussion

Two questions were posed for this portion of the analysis:

- 1) What is the groundwater recharge area to the landslide?
- 2) What is the relative importance of bank erosion into the toe of the slope verses increases in groundwater flux to the slope for initiating and or accelerating movement of the landslide?

With existing information, we used simulation models to address both. The answer to the first is straightforward: the model clearly delineates a recharge area. The answer to the second must be inferred from calculations of sensitivity. We predict that bank erosion is the predominant factor at the base of the slope, but that both processes act over the body of the landslide. We find, however, that each process affects different portions of the landslide. We've also highlighted a third, perhaps equally important process: fluvial erosion of material from channels draining the landslide. These results are functions of the data and model we used. We've gathered little new information for this project; we've simply capitalized on our understanding of the processes involved to infer answers consistent with the information we have. Results must be interpreted in light of the limitations of these data, acknowledging that, without new information, that may be the best we can do.

Inference and simplification is inherent in construction of any model. We can take steps to limit the influence of uncertainty, as we've done in examining the sensitivity of our calculations to change (using Equation (1)), rather than direct measures of stability (the factors of safety). Unfortunately, an estimate of sensitivity may not translate directly into an answer to question 2. A highly sensitive slope may still not fail if its inherent stability is high; conversely, a slope of low sensitivity may fail if its inherent stability is low. We must interpret measures of sensitivity in light of actual slope stability (as we've tried to do in part by imposing an upper limit to the factor of safety for grid cells included in the calculation of sensitivity). We can use the calculated stability as shown in Figure 3.4, but the problems with unresolved spatial heterogeneity can leave those predictions unreliable. In the end, we must base our confidence in model results on their ability to explain observed landslide behavior. To do that, we must also factor in time, since landslide response depends not only on its sensitivity to particular changes, but also on the timing and persistence of those changes.

Temporal Patterns of Slope Stability

Having used steady-state analyses and the topography from a particular date in 1978, we have essentially examined one point in time. Yet we know that landslide response varies as conditions change. The spatial patterns of sensitivity explored above implicitly include a temporal component, since the perturbations we've examined involve a change over time, either a change in pore pressures or a change of landslide topography. Here we examine the role of changing pore pressures directly, using the simulated time series of recharge and transient groundwater analyses.

The aquifer is continuously depleted as groundwater is discharged at surface seeps and drained overland in stream channels; it is recharged by water infiltrating the soil during periods of precipitation. Thus the volume of water stored in the aquifer fluctuates continuously with corresponding fluctuations in groundwater flow and pore pressures. These fluctuations are simulated with a transient groundwater analysis and are shown for a single year in Figure 3.10. (This analysis differs from others discussed in this report in that groundwater flow was simulated

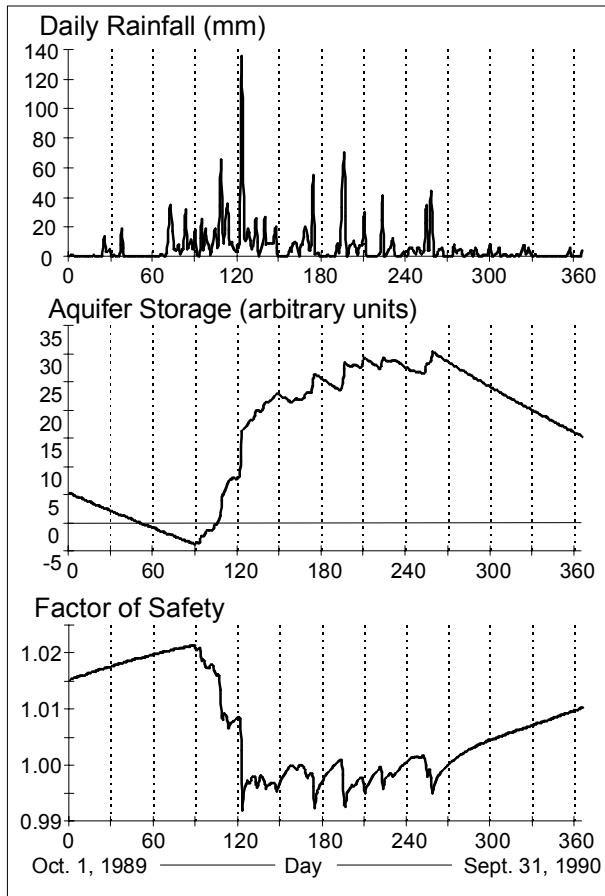


Figure 3.10. Precipitation, aquifer storage, and stability of one transect over the course of a single year. Note that the volume of water in storage is greater at the end of the period than at the start.

shorter than indicated here. It is also a function of aquifer geometry: the greater the distance water must flow, and the larger the proportion of area receiving recharge relative to that discharging water to the surface, the longer the response time of the aquifer. Hence the length of aquifer “memory” will vary over the body of the landslide relative to the shape and size of the recharge area to each particular zone.

We’ve plotted factor-of-safety time series for both forested and clearcut simulations. The transect chosen is sensitive to changes in pore pressures and shows a decrease in stability for clearcut conditions, relative to fully forested. The change is quite small, a decrease in the factor of safety of only about 1%, but it is instructive to examine the consequences of this change over time. Suppose for a moment that the absolute value of the predicted factor of safety is accurate. Then every time it dips below a value of one, the slope fails. This transect traverses a slope showing evidence of persistent movement on a series of poorly defined slumps that evolve, in places, into mud flows. Failure, in this case, entails a balance of forces that allows slowdownslope movement of this debris.

only along a single transect, which was placed along a flow path within the recharge area as determined with the steady-state analysis. Comparison with a short-term simulation using the entire model indicated no substantial discrepancies.) Storage increases during periods of precipitation and gradually decreases otherwise. The aquifer fills up much more quickly than it empties out. Using the simulated water table, we’ve also calculated the factor of safety along a single transect for each day of the year. Stability along this transect varies inversely with the volume of aquifer storage.

Figure 3.11 shows a daily time series of aquifer storage and factor of safety along the same transect for the entire 60-year precipitation record. We’ve also plotted the total annual depth of precipitation for each water year. This long simulation illustrates an important point: slope response in any year is conditioned by aquifer storage, which may depend on antecedent precipitation extending several years back. Model results suggest that a series of marginally wet years may raise water table levels and destabilize slopes, greatly exacerbating the effects of another wet year. A series of dry years may lower water table levels and modulate the effects of a subsequent wet year. Likewise, the effects of a change in vegetation within the recharge area may take several years to be manifest at the landslide itself. The length of this “memory” is a function of the specific yield and saturated conductivity values assigned to the aquifer and may be longer or

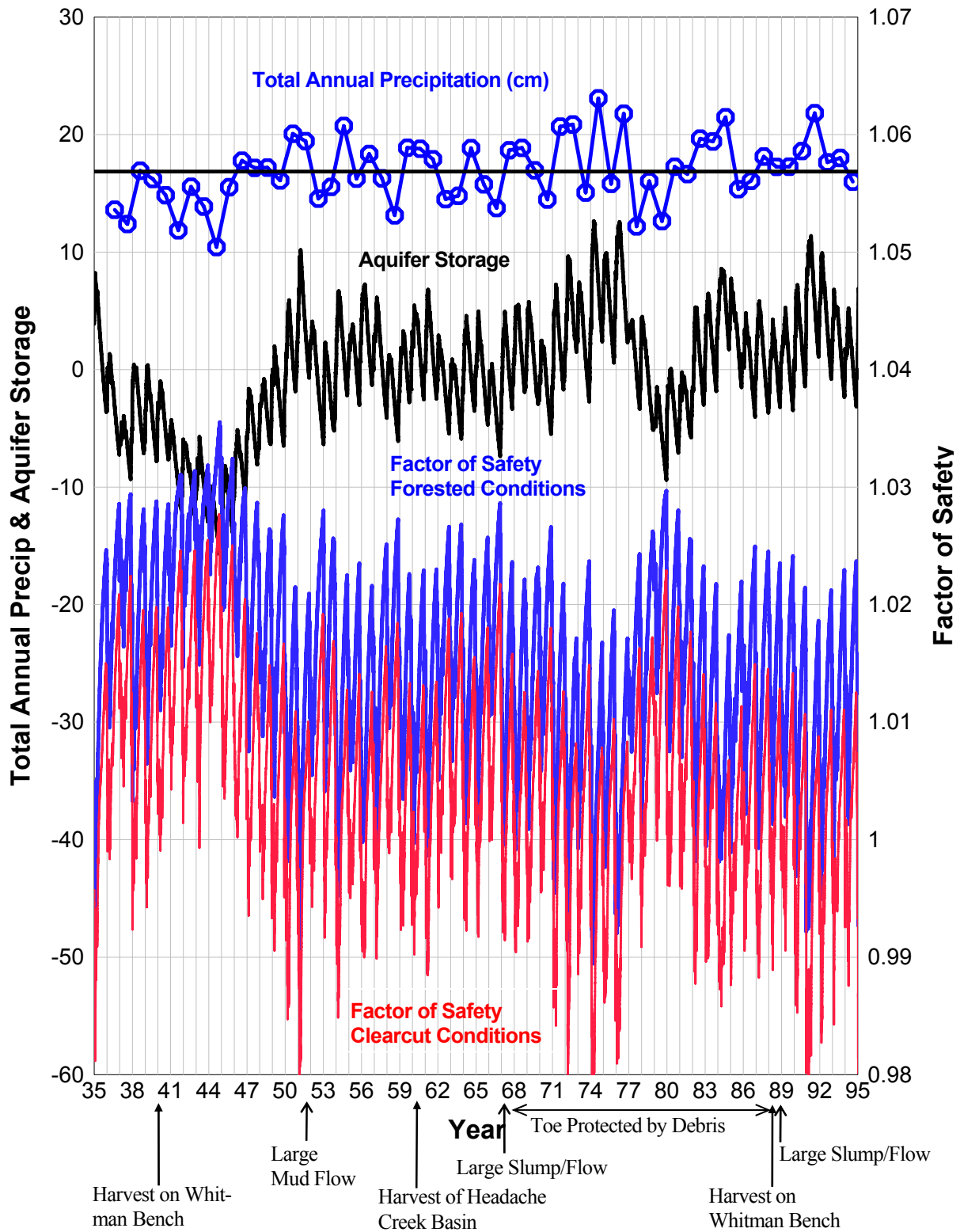


Figure 3.11. 60-year time series.

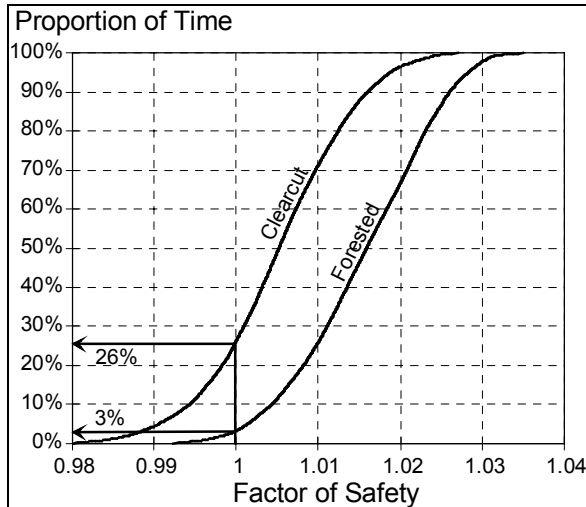


Figure 3.12. Cumulative frequency distribution of simulated stability for a single slope.

used, with more data) and better answers may be found with additional effort. In any case, the confidence we place in a model or set of analysis methods ultimately depends on how useful we find them for explaining and anticipating landslide behavior.

Landslide history was described in Section 1. The photographs and tracings shown in Figure 1.4 illustrate landslide activity over the last 50 years. The major events are indicated along the time line of Figure 3.11. Calculations were made with 1978 topography, so some interpretation is required in applying these predictions to the landslide over time. The 1967 event dramatically altered the surface geometry of the landslide and calculated stability and sensitivity will not apply prior to that time. Areas of activity indicated in the post 1970 photographs and prior to 1990 fall within areas indicated to be sensitive both to increases in recharge and to incision of channels draining the body of the landslide. The major activity since 1990 has occurred in areas primarily sensitive to cutting of the toe.

Effects of Toe Cutting

Landslide history clearly indicates great dependence on conditions at its base along the Stillaguamish River. Big, river-moving events have occurred only when the channel impinges on the toe. No large events took place during the rather wet years of the early and mid seventies (see Figure 3.11) when the toe was protected by debris from the 1967 event. It was not until 1988, when that debris was eroded away and the river again had access to the toe of the landslide, that large-scale slumping reoccurred. Even during times of apparent quiescence, however, activity persists upslope, as shown by the persistent appearance of exposed headscarps and unvegetated areas in the 1978, 1984, and 1988 photographs. These observations correlate well with predictions of landslide sensitivity. The calculated effects of toe erosion are twice as great as those of increased recharge or channel incision and the zones of observed activity match well with those predicted to be sensitive to toe cutting.

Effects of Harvest

Of equal importance, but less amenable to interpretation, are apparent correlations between harvest in the groundwater recharge area and movement of the landslide. Benda et al. (1988) noted (1) the increase of landslide activity in the early 1950s following harvest on Whitman Bench in 1940 and (2) the increase of landslide activity in the mid 1960s following harvest of the Headache Creek Basin in 1960. We now add (3) slumping in the western portion of the landslide shown in the 1991 photograph following timber harvest within the ground-

Hence, the extent of movement, and the volume of material moved to the channel, depends not only on the frequency that the factor of safety dips below unity, but also on the total length of time it spends there. From these time series we produce a cumulative frequency distribution for both cases, shown in Figure 3.12. In the forested simulation, the factor of safety is less than unity about 3% of the time, as compared to 26% of the time for the clearcut simulation. Clearly, time must be factored into our analysis. The sensitivities to changing recharge shown in Figure 3.6 do not tell the whole story: a small change, integrated over time, can have large consequences.

Empirical Comparison

There is no fail-proof test of these methods. The results presented are based on limited data and simple models. We've tailored the realism of the models to the data we have (vastly more complex models could certainly be

water recharge area on Whitman Bench sometime between 1987 and 1991. We must examine these correlations in relationship to the pattern of annual precipitation and conditions at the landslide toe. In all three cases, the Stillaguamish was actively eroding the landslide toe. The first and third (1950s and 1990s) occurred during periods of unusually high annual precipitation (Figure 3.11). The second period of activity (1960s), however, occurred during a period of relatively average precipitation. These factors confound easy interpretation.

The simulated time series in Figure 3.11 show that the aquifer may take several years to respond to changes in recharge. As we discussed, the length of this time lag is a function of both aquifer properties and of aquifer geometry and may vary for different portions of the landslide. Hence, we can expect some years delay between the occurrence of harvest and any recharge-related effects of harvesting. We must also examine the impact of a harvest-related change in recharge relative to effects of annual variation in precipitation. We can use Figure 3.11 for this purpose as well. Under forested conditions we predict a variable state of stability as shown by the blue factor-of-safety line. Harvesting of the recharge area causes stability to shift, over the course of several years, to the red line. As the forest regrows, the time-series of stability gradually shifts, over the course of decades, back to the blue line. Although the change is minor, a small reduction in slope stability may increase the probability of failure over time and, as shown in Figure 3.12, can increase the frequency and total time for displacement of slow-moving slumps and mud flows.

We can also compare the location of harvest to the subsequent locus of activity on the landslide. Harvest of Headache Creek basin, as occurred around 1960, should primarily affect the east-central portion of the landslide (the orange zone in Figure 3.2), correlating with the location of the large 1967 event. Harvest of the Whitman Bench, as occurred in the late 1980s, should primarily affect slopes through the west and west-central portions of the landslide (yellow and purple zones in figure 3.2), correlating with activity in the 1990s. Based on model results we anticipate both temporal and spatial correlation of harvest and accelerated landslide activity, as observed.

Recharge on Steep, Bedrock Slopes with Thin Soils versus Low-Gradient Slopes with Thick Soils

This is the third question posed by the Level 1 analysis team. Since field observations indicated that groundwater recharge to the Hazel slide did not extend beyond Whitman Bench, this issue was not addressed directly with the numerical analysis. The flow of water over steep, bedrock slopes with thin soils involves a mechanism not included in the models presented here: shallow subsurface flow. For well-drained sites, differences in evapotranspiration between two such sites may be minor, as discussed in Section 2. However, the flow paths of water infiltrating the soil may be quite different. At a low-gradient site with deep soils, water may percolate directly to groundwater. On steep, bedrock slopes the permeability contrast between soil and bedrock, and the steep gradient of this contact, will tend to keep water above the contact, causing saturated flow within the soil. Where the level of saturation intersects the surface, water exfiltrates and flows overland to channels as subsurface return flow. There is less opportunity for infiltration to deep groundwater, so it is likely that recharge from such sites will be minimal. In reference to recharge in bedrock areas upslope of Whitman Bench, however, note the extensive low-gradient areas at the top of the slope (Figure 1.1). These areas compose the headwaters of Rollins and Deer Creeks, and offer ample opportunity for infiltration into the bedrock.

Summary

These results indicate that toe erosion is the primary factor initiating the spectacular, river-moving events that everyone notices. (One caveat: the large event of 1967 altered landslide topography to an extent that these results, based on 1978 topography, may not apply for periods prior to 1967. The groundwater flow field and recharge area would not be greatly influence by this change, but calculated stability and sensitivity may be greatly influenced. It may be that the landslide prior to 1967 was much more sensitive to changes in recharge, and that the 1967 event occurred in response to harvest of the Headache Creek basin.) Harvest activity in the recharge area can reduce stability of these same slopes and the model predicts the type of temporal and spatial correlations observed between harvesting and accelerated landslide activity. However, the magnitude of effects of harvest on slope stability are less than those associated with bank erosion. We surmise that harvest-related reduc-

tions in stability can affect the timing and increase the size of any single failure, but that such failures would still occur in the absence of harvest solely in response to erosion of the toe.

Headward expansion of the landslide is indicated to occur in response to all three factors: erosion of the toe, increases of pore pressure, and incision of channels draining the body of the landslide. Each factor, however, affects certain portions of the landslide. In particular, expansion towards Headache Creek occurs in response to toe cutting and channel incision. Although the headscarp in that area remains active, headward expansion towards Headache Creek since 1970 (as inferred from its position on the photograph) has been minor. This in no way implies, however, that the potential does not exist. Indeed, tension cracks and steps north of the active scarp suggest that new slumps continue to develop. We surmise that these slumps will continue to move in response to erosion of material from their toes by the channels draining the landslide.

Chronic delivery of fine-grained sediment to the Stillaguamish occurs both from bank failures and from flushing of fines by the streams draining the body of the landslide. These groundwater-fed streams flow year round; their primary sources of sediment are persistent small slumps and flows adjacent to their channels. Calculations indicate that these mass-wasting features respond both to increases in pore pressure and to erosion of material from the channels at their toes. Harvest-related increases in groundwater recharge can reduce stability of some of these slopes, as shown in Figure 3.6. Likewise, any increases in groundwater recharge will increase discharge through the landslide-draining streams. Although not examined in this analysis, increased discharge may increase transport of fine-grained material off of the landslide, with correspondingly greater rates of channel incision. Hence, we surmise that increased groundwater flux related to harvest will increase chronic delivery of fine-grained material into the Stillaguamish River.

Resources and Tasks Required for Similar Analyses

This analysis was done on a high-end PC (Pentium Pro, 64Mbytes of memory). The drawback of using a low-cost computer (relative to a scientific workstation) is that computational times are rather prolonged, several days for a single transient analysis. This is a minor drawback, since we couldn't perform any analysis at all if we couldn't afford the computer. We used inexpensive software. The finite-element groundwater model is available free from the USGS; the geographic information system IDRISI is available for under \$1000 from Clark University; graphics were composed using a spreadsheet (Microsoft Excel) and a drawing program (Micrographx Designer); additional code was written in FORTRAN and compiled with Microsoft Powerstation, Version 4.0.

The data needs of the evapotranspiration simulation are described in Section 1. The groundwater and slope stability analyses require high resolution topographic data, preferably digital line graphs of 20-foot contours from 1:4800-scale mapping from which a 10-meter (or smaller) grid can be constructed. Subsurface stratigraphy must be inferred from careful mapping of surface exposures. Well and borehole logs would be invaluable. Zones of surface saturation and seepage must also be carefully mapped, preferably at the end of both wet and dry seasons, to calibrate the groundwater model. Monitor-well logs could also be used for this purpose. Surface transects and field-based cross sections are required for back-calculating strength parameters (cohesion and angle of internal friction) for material composing the slopes. All aquifer and geotechnical properties are further constrained by values reported in the literature for similar materials. A sequence of aerial photographs at periodic intervals and spanning several decades is desirable for testing of model predictions.

This work involved an initial application of these analysis tools, many of which were developed specifically for this project. It is quite feasible to extend their applicability in future projects. We have not fully utilized the spatially distributed capabilities of the models. One could, for example, model explicitly the effects of specific harvest plans, simulating the effects of spatially limited harvest units and regrowth over time.



References

- Benda, L., G. W. Thorsen, and S. Bernath, 1988, *Report of the I.D. team investigation of the Hazel Landslide on the North Fork of the Stillaguamish River (F.P.A. 19-09420)*, Department of Natural Resources, Northwest Region, Sedro Woolley, 13 p. plus 2 figures*
- Bishop, A. W., 1955. The use of the slip circle in the stability analysis of slopes, *Geotechnique*, Vol. 5, pp. 7-17.
- Buxton, H.T., and Modica, E., 1992, Patterns and rates of ground-water flow on Long Island, New York: *Ground Water*, v. 30, no. 6, p. 857-866
- Cooley, R.L., 1992, A MODular Finite-Element model (MODFE) for areal and axisymmetric ground-water-flow problems, part 2—derivation of finite-element equations and comparisons with analytical solutions: U.S. Geological Survey Techniques of Water-Resources Investigations, book 6, chap. A4.
- Czarnecki, J.B., and Waddell, R.K., 1984, Finite-element simulation of ground-water flow in the vicinity of Yucca Mountain, Nevada-California: U.S. Geological Survey Water-Resources Investigations Report 84-4349, 38 p
- DNR, in prep. Hazel Watershed Analysis, Washington State, Watershed Analysis Report, Department of Natural Resources, Northwest Region, Sedro Woolley
- Iverson, R.M., and Reid, M.E., 1992, Gravity-driven groundwater flow and slope failure potential, 1. Elastic effective-stress model: *Water Resources Research*, v. 28, no. 3, p. 925-938.
- Koloski, J.W., S. D. Schwarz, and D. W. Tubbs, 1989, Geotechnical properties of geologic materials, in R. W. Galster (ed), *Engineering Geology in Washington*, Volume 1, Bulletin 78, Washington Division of Geology and Earth Resources, Department of Natural Resources, p.19-26.
- Palladino, D. J., and R. B. Peck, 1972, Slope failures in an overconsolidated clay, Seattle, Washington, *Geotechnique*, vol. 22, p. 563-595.
- Miller, D. J., 1995, Coupling GIS with physical models to assess deep-seated landslide hazards, *Environmental & Engineering Geoscience*, vol. 1, pp263-276.
- Reid, M.E., and Iverson, R.M., 1992, Gravity-driven groundwater flow and slope failure potential, 2. Effects of slope morphology, material properties, and hydraulic heterogeneity: *Water Resources Research*, Vol. 28, p. 939-950.
- Shannon, W. D., and Associates, 1952, *Report on slide on North Fork Stillaguamish River near Hazel, Washington*, to the State of Washington Departments of Game and Fisheries, 18 pp. plus appendix by H. Coombs, 8 plates*
- Thorsen, G. W., 1969, Memorandum: Landslide of January 1967 which diverted the North Fork of the Stillaguamish River near Hazel, to M. T. Huntting, supervisor, 7 pp.*
- Thorsen, G. W., 1989, Landslide provinces in Washington, in R. W. Galster (ed), *Engineering Geology in Washington*, Volume 1, Bulletin 78, Washington Division of Geology and Earth Resources, Department of Natural Resources, p. 71-89.
- Torak, L.J., Davis, G.S., Herndon, J.G., and Strain, G.A., 1992, Geohydrology and evaluation of water-resource potential of the upper Floridan aquifer in the Albany area, southwestern Georgia: U.S. Geological Survey Water-Supply Paper 2391, 59 p.

* on file with the Department of Natural Resources, Northwest Region, Sedro Woolley

- Torak, L.J., 1993a, A MODular Finite-Element model (MODFE) for areal and axisymmetric ground-water-flow problems, part 1—model description and user's manual: U.S. Geological Survey Techniques of Water-Resources Investigations, book 6, chap. A3.
- Torak, L.J., 1993b, A MODular Finite-Element model (MODFE) for areal and axisymmetric ground-water-flow problems, part 3—design philosophy and programming details: U.S. Geological Survey Techniques of Water-Resources Investigations, book 6, chap. A5.
- Wolff, N., 1988, Memorandum to Summit Timber Company (FPA #1909420) concerning the Hazel Landslide, 3 pp.*
- Wolff, N., M. Nystrom, and S. Bernath, 1989, *The effects of partial forest-stand removal on the availability of water for groundwater recharge*, report submitted to H. Villager, Northwest Regional Manager, Department of Natural Resources, 14 pp.*

* on file with the Department of Natural Resources, Northwest Region, Sedro Woolley

Addendum: Effects of Clearcutting Outside of the Groundwater Recharge Area

The original analysis applied spatially uniform recharge. This allowed us to examine the effects of variability in time without the added complication of variability in space. Here we examine briefly the effects of spatially variable recharge. We find that clearcutting outside of the groundwater recharge area can slightly increase flow of groundwater to the landslide. Examination of the results suggest, however, that effects of clearcutting vary with position: clearcutting east of the landslide will lower stability of eastern slopes, clearcutting north of the recharge area will affect a small area in the northwest portion of the landslide, clearcutting west of the recharge area appears to have no effect.

The spatial pattern of recharge effects the spatial pattern of groundwater flow. Regions of high recharge can locally elevate the watertable, whereas regions of low recharge can locally lower the watertable. Spatial variations in vegetation cover, and associated rates of recharge, can thereby influence the pattern of groundwater flow. For example, clearcutting outside of the groundwater recharge area to the Hazel landslide will locally raise water tables, which may extend the recharge area and increase groundwater flux to the landslide. We examine that effect here and calculate the potential effect on stability of the landslide.

The simplest case is that of maintaining complete forest cover over the recharge area identified in Figure 3.2 and clearcutting of all areas outside. We apply this scenario in a steady-state (time-averaged) analysis with the largest estimated mean recharge for the clearcut and the lowest estimated mean recharge for the forest. We thus use the estimates giving the largest difference in recharge between forested and clearcut conditions. This is the ‘worst-case scenario’ for landslide stability; all other estimates should produce reductions in stability less than obtained here.

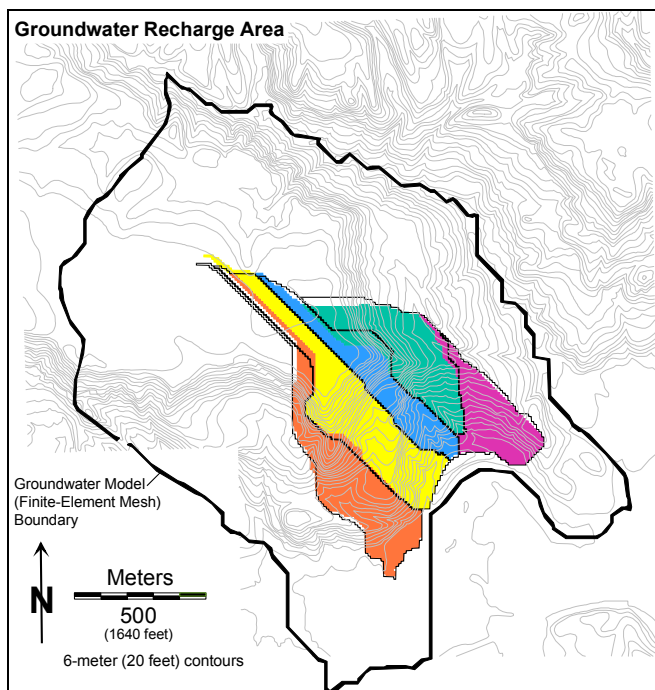


Figure 3.13. Effects of clearcutting outside of the groundwater recharge area to the Hazel slide. The colored polygons show the recharge area estimated with a spatially uniform recharge (the same as shown in Figure 3.2); the black lines delineate the recharge area estimated with simulated clearcutting outside of the colored polygons. The increase in recharge to the landslide is small. As in Figure 3.2, the polygons delineate distinct and separate regions of groundwater flow to the landslide.

The groundwater model indicates that clearcutting outside of the recharge area identified in Figure 3.2 causes a general increase in watertable levels over Whitman Bench. The predicted increase in groundwater flow to the landslide, however, is small. Figure 3.13 shows the predicted change in the groundwater recharge area to the landslide. Clearcutting of all uncolored zones within the model boundary cause only a minor increase in the groundwater recharge area to the slide, with expansion occurring mostly to the north.

The increased groundwater flow to the landslide, although small, does nevertheless influence slope stability. This influence is estimated through a calculation of sensitivity using Equation 1. Results are shown in Figure 3.14. We find reductions in the calculated factor of safety of the same magnitude as those obtained by going from entirely forested to entirely clearcut conditions (Figure 3.6), with reductions in some areas approaching 30%. The spatial extent of these reductions is considerably smaller than that found when the recharge area is also clearcut (shown in Figure 3.6b for the recharge values used here).

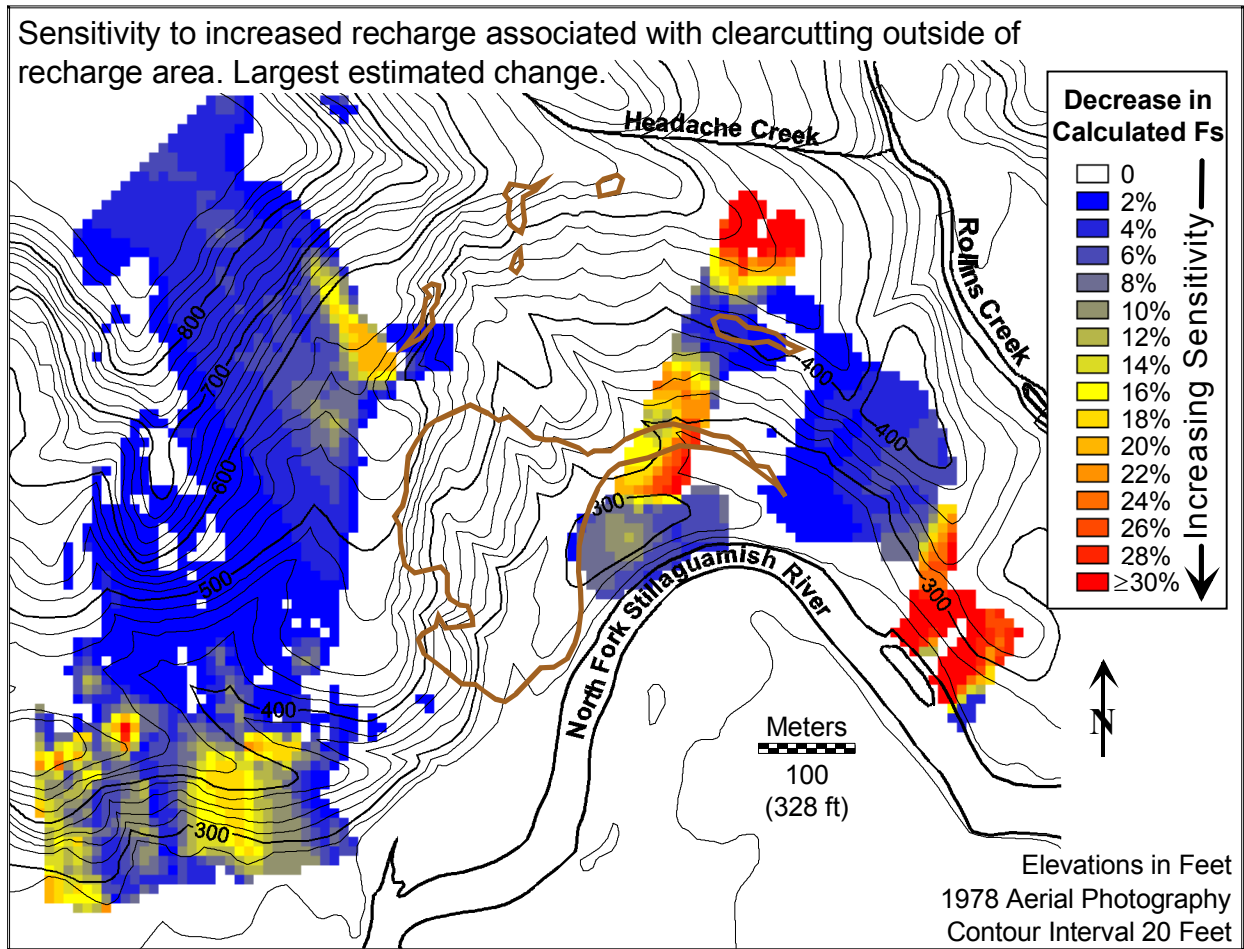


Figure 3.14. Sensitivity to clearcutting outside of the groundwater recharge area to the landslide. Two areas of sensitivity on the landslide are identified, the southwest-facing slopes over the eastern portion of the slide and a smaller zone on the northern edge of the bench on the western portion of the landslide. These results are obtained using the greatest estimated recharge for clearcut areas and the smallest estimated recharge for forested areas and so represent the largest estimated reduction in stability.

We may make some inferences as to the effects of increasing recharge over smaller areas than simulated here. Figure 3.14 shows two major areas of sensitivity within the landslide, the southwest-facing slopes on the eastern portion of the landslide and an area on the northern edge of the bench on the western portion of the landslide. Figure 3.13 shows that the eastern slopes receive groundwater only from Headache Creek basin and areas east; the bench receives groundwater from areas to the northwest, including the eastern portion of Whitman Bench north of the recharge area. Clearcutting of areas on Whitman Bench west of the recharge area do not appear to have any influence on stability of the landslide itself.